

แผ่นเส้นใยอิเล็กทรอนิกส์เป็นแก๊สเซนเซอร์เชิงแสงสำหรับฟอร์มาลดีไฮด์

นางสาวจุฑิตรีรัตน์ หลักบุญ

วิทยานิพนธ์นี้เป็นส่วนหนึ่งของการศึกษาตามหลักสูตรปริญญาวิทยาศาสตรมหาบัณฑิต  
สาขาวิชาปิโตรเคมีและวิทยาศาสตร์พอลิเมอร์  
คณะวิทยาศาสตร์ จุฬาลงกรณ์มหาวิทยาลัย  
ปีการศึกษา 2555  
ลิขสิทธิ์ของจุฬาลงกรณ์มหาวิทยาลัย

บทคัดย่อและแฟ้มข้อมูลฉบับเต็มของวิทยานิพนธ์ตั้งแต่ปีการศึกษา 2554 ที่ให้บริการในคลังปัญญาจุฬาฯ (CUIR)  
เป็นแฟ้มข้อมูลของนิสิตเจ้าของวิทยานิพนธ์ที่ส่งผ่านทางบัณฑิตวิทยาลัย

The abstract and full text of theses from the academic year 2011 in Chulalongkorn University Intellectual Repository (CUIR)  
are the thesis authors' files submitted through the Graduate School.

ELECTROSPUN FIBER MATS AS OPTICAL GAS SENSOR  
FOR FORMALDEHYDE

Miss Thitirat Lukboon

A Thesis Submitted in Partial Fulfillment of the Requirements  
for the Degree of Master of Science Program in Petrochemistry and Polymer Science  
Faculty of Science  
Chulalongkorn University  
Academic Year 2012  
Copyright of Chulalongkorn University

Thesis Title	ELECTROSPUN FIBER MATS AS OPTICAL GAS SENSOR FOR FORMALDEHYDE
By	Miss Thitirat Lukboon
Field of Study	Petrochemistry and Polymer Science
Thesis Advisor	Luxsana Dubas, Ph.D.
Thesis Co- Advisor	Ratthapol Rangkupan, Ph.D.

---

Accepted by the Faculty of Science, Chulalongkorn University in Partial  
Fulfillment of the Requirements for the Master's Degree

..... Dean of the Faculty of Science  
(Professor Supot Hannongbua, Dr.rer.nat.)

#### THESIS COMMITTEE

..... Chairman  
(Assistant Professor Warinthorn Chavasiri, Ph.D.)

..... Thesis Advisor  
(Luxsana Dubas, Ph.D.)

..... Thesis Co- Advisor  
(Ratthapol Rangkupan, Ph.D.)

..... Examiner  
(Associate Professor Voravee Hoven, Ph.D.)

..... External Examiner  
(Pramee Pengprecha, Ph.D.)

ฐิติรัตน์ หลักบุญ : แผ่นเส้นใยอิเล็กโทรสปินเป็นแก๊สเซนเซอร์เชิงแสงสำหรับฟอร์มัลดีไฮด์  
(ELECTROSPUN FIBER MATS AS OPTICAL GAS SENSOR FOR FORMALDEHYD)

อ.ที่ปรึกษาวิทยานิพนธ์หลัก: อ.ดร.ลักขณา คูบาส , อ.ที่ปรึกษาวิทยานิพนธ์ร่วม: อ.ดร.รัฐพล รังกุพันธุ์, 68 หน้า.

การพัฒนาเซนเซอร์เพื่อตรวจวัดแก๊สฟอร์มัลดีไฮด์ที่สามารถมองด้วยตาเปล่าได้ โดยใช้สารผสมระหว่างพอลิเมอร์/ซีพีเอฟเอเจนต์/น้ำมิลลิคว ซึ่งได้เตรียมเซนเซอร์ โดยใช้เทคนิค อิเล็กโทรสปินนิ่งและเทคนิคการฉาบ เมื่อซีพีเอฟเอเจนต์ทำปฏิกิริยากับแก๊สฟอร์มัลดีไฮด์ จะเปลี่ยนสีจากสีเหลืองเป็นสีม่วงและปรากฏค่าการดูดกลืนแสงสูงสุดที่ 580 นาโนเมตร สันฐานวิทยาของเส้นใยที่เกิดขึ้นจากกระบวนการอิเล็กโทรสปินนิ่งถูกวิเคราะห์ด้วยกล้องจุลทรรศน์แบบใช้แสงและกล้องจุลทรรศน์อิเล็กตรอนแบบส่องกราด ในการศึกษาครั้งนี้ ได้ศึกษาพอลิเมอร์สองชนิดคือ พอลิเอทิลีนออกไซด์และพอลิไวนิลแอลกอฮอล์ สภาวะที่เหมาะสมในกระบวนการอิเล็กโทรสปินนิ่ง ได้มีการใช้อัตราส่วนของพอลิไวนิลแอลกอฮอล์ /ซีพีเอฟเอเจนต์/น้ำมิลลิคว ที่อัตราส่วน 10/90/0 โดยมีการควบคุมอัตราการไหลของไซริงค์ปั๊มที่ 0.1 มล./ชม., ความต่างศักย์ไฟฟ้า 20 กิโลโวลต์ และระยะห่างระหว่างปลายเข็มถึงฉากรับเส้นใยที่ 25 ซม. พบว่าแผ่นเส้นใยพอลิไวนิลแอลกอฮอล์ / ซีพีเอฟเอเจนต์/ น้ำมิลลิคว นั้นให้ลักษณะเส้นใยมีความสม่ำเสมอ และมีขนาดเส้นผ่านศูนย์กลางของเส้นใยที่  $342 \pm 41$  นาโนเมตร ในการศึกษาครั้งนี้ แก๊สฟอร์มัลดีไฮด์ถูกสร้างขึ้นโดยให้อุณหภูมิและการเขย่า ในขณะเดียวกันได้ปล่อยแก๊สไนโตรเจนลงในสารละลายฟอร์มัลดีไฮด์ ลำดับแรก สภาวะของการสร้างแก๊สฟอร์มัลดีไฮด์ต้องเหมาะสม ส่วนอุณหภูมิและอัตราการคนสารละลายที่เหมาะสมคือ 50 องศาเซลเซียสและ 100 รอบ/นาที ตามลำดับ อิเล็กโทรสปินเซนเซอร์และฟิล์มเซนเซอร์ถูกนำมาใช้ในการตรวจวัดแก๊สฟอร์มัลดีไฮด์ที่สร้างขึ้น ที่ช่วงความเข้มข้น 61–122 ไมโครกรัมต่อลิตร ค่าเบี่ยงเบนมาตรฐานสัมพัทธ์ของค่าการดูดกลืนแสงที่ 580 นาโนเมตร ของอิเล็กโทรสปินเซนเซอร์และฟิล์มเซนเซอร์ คือ ร้อยละ 1.22 และร้อยละ 2.66 ตามลำดับ

สาขาวิชา ปิโตรเคมีและวิทยาศาสตร์พอลิเมอร์ .....  
ปีการศึกษา 2555 .....

ลายมือชื่อ อ.ที่ปรึกษาวิทยานิพนธ์หลัก.....  
ลายมือชื่อ อ.ที่ปรึกษาวิทยานิพนธ์ร่วม.....

# # 537 25314 23: MAJOR PETROCHEMISTRY AND POLYMER SCIENCE  
KEYWORDS: SCHIFF'S REAGENT/ ELECTROSPINNING/ FORMALDEHYDE  
SENSING

THITIRAT LUKBOON: ELECTROSPUN FIBER MATS AS OPTICAL  
GAS SENSOR FOR FORMALDEHYDE. ADVISOR: LUXSANA DUBAS,  
Ph.D., CO-ADVISOR: RATTHAPOL RANGKUPAN, Ph.D., 68 pp.

The developed sensor for detecting a formaldehyde gas by visual detection using a mixture of polymer solution/Schiff's reagent/Milli-Q water was prepared by the electrospinning and film casting techniques. When Schiff's reagent was exposed to formaldehyde gas, its color changed from yellow to violet and appeared absorbance  $\lambda_{\max}$  at 580 nm. Morphology of electrospun fibers was characterized by Optical Microscope (OM) and Scanning Electron Microscope (SEM). In this experiment, two types of studied polymer sensor: polyethylene oxide (PEO) and polyvinyl alcohol (PVA) were investigated. The optimized condition of electrospinning process were the 10:90:0 mass ratio of PVA/Schiff's reagent/Milli-Q water, flow rate of syringe pump was 0.1 mL/hr, electric field of 20 kV, and distance between needle and collector of 25 cm. It was found that the obtained size of PVA/Schiff's reagent/Milli-Q water electrospun fibers appeared to be well-distributed, and its diameter is in a range of  $342 \pm 41$  nm. In this study, the formaldehyde gas was generated using temperature and agitation as well as bubbling with nitrogen gas in to the formalin solution. First, the condition of generating formaldehyde gas system is optimized. The optimized temperature and stirring rate are 50 °C and 100 rpm, respectively. The electrospun sensor and film sensor were used to detect the generated formaldehyde gas concentration in a range of 61-122  $\mu\text{g/L}$ . The relative standard deviation (%RSD) of the absorbance at 580 nm of both electrospun sensor and film sensor are 1.22% and 2.66%, respectively.

Field of study Petrochemistry and Polymer Science. Student's Signature

Academic Year: 2012..... Advisor's Signature.....

Co- advisor's Signature.....

## ACKNOWLEDGEMENTS

I would like to express my gratitude to all those who made the completion of this thesis possible. First of all, I wish to express highest appreciation to my thesis advisor, Dr. Luxsana Dubas, for her suggestions, assistance, constructive, inspiration, and strong support throughout the duration of my thesis. I am deeply indebted to her valuable guidance, understanding and patience. I would also like to thank my co-advisor, Dr. Ratthapon Rangkupan for his beneficial advice and encouragement which had a great benefit through my thesis work. In addition, I am also grateful to Asst. Prof. Dr. Warinthorn Chavasiri, Assoc. Prof. Voravee Hoven and Dr. Pramee Pengprecha for their valuable suggestions and comments as committee members and thesis examiners.

This thesis cannot be completed without kindness and helps from many people. I would like to thank the Chromatography and Separation Research Unit for the facilities. The friendship and support from group members are invaluable. I wish to express my sincere thanks to Dr. Stephan T. Dubas, and Miss Apisaranut Sangkaong for their helpful recommendations and encouragement. I would like to thank Mr. Taweesak Chanduang and Acting Sub Lt. Sira Nitiyanontakit for all his assistance in building all equipments. Furthermore, I would sincere thank to all members of Chromatography and Separation Research Unit (ChSRU) for their helpfulness, kindness, lovely friendship, encouragement and valuable suggestions; especially all members of 1253 Laboratory.

Finally, I would like to thank my heartfelt gratitude goes to my beloved family; father, mother, my sister and my intimate friends for all their love, understanding and support.

## CONTENTS

	<b>Page</b>
ABSTRACT (IN THAI).....	iv
ABSTRACT (IN ENGLISH).....	v
ACKNOWLEDGEMENTS.....	vi
CONTENTS.....	vii
LIST OF TABLES.....	xi
LIST OF FIGURES.....	xii
LIST OF ABBREVIATIONS AND SYMBOLS.....	xv
<b>CHAPTER I INTRODUCTION.....</b>	<b>1</b>
1.1 Research Objective.....	3
1.2 Scopes of this research.....	3
1.3 The benefit of this research.....	3
<b>CHAPTER II THEORY AND LITERATURE REVIEW.....</b>	<b>4</b>
2.1 Formaldehyde.....	4
2.1.1 Properties.....	4
2.2 Schiff's reagent.....	5
2.3 Electrospinning technique.....	7
2.3.1 The main equipment used in the electrostatic fiber spinning.....	8
2.3.2 Principles of spinning fibers.....	9
2.3.3 Mechanism of the fiber.....	10
2.3.4 Factors influencing the fiber spinning.....	11
2.3.5 Properties of nanofibers.....	12
2.4 Casting technique.....	12
2.5 Literature review.....	12

	<b>Page</b>
<b>CHAPTER III EXPERIMENTAL</b> .....	16
3.1 Apparatus.....	16
3.2 Chemicals.....	18
3.2.1 Preparation of reagents.....	19
3.2.1.1 Schiff's reagent solution.....	19
3.2.1.2 The mixture of polymer media/Schiff's reagent/Milli-Q water solution.....	19
3.2.1.3 0.8% v/v acetylacetone solution.....	20
3.2.1.4 Formaldehyde solution.....	20
3.3 Sensor fabrication.....	20
3.3.1 Electrospinning process.....	20
3.3.1.1 Effect of weight ratio of PEO/Schiff's reagent/Milli-Q water on the morphology of electrospun fiber.....	21
3.3.1.2 Effect of weight ratio of PVA/Schiff's reagent/Milli-Q water on the morphology of electrospun fiber.....	22
3.3.1.3 Optimization of the parameters of the electrospinning process..	23
3.3.2 Casting process.....	24
3.4 Characterization .....	24
3.4.1 Solution viscosity.....	24
3.4.2 Solution conductivity.....	25
3.4.3 Morphology of electrospun fiber.....	25
3.5 Study of sensor stability.....	25
3.5.1 Thermal stability.....	25
3.5.2 Time stability.....	26
3.6 Process of generating formaldehyde gas.....	26
3.6.1 Reaction time.....	27
3.6.2 Working time.....	28
3.6.3 Effect of temperature.....	29



	<b>Page</b>
3.6.4 Effect of stirring rate.....	29
3.7 Determination of generated formaldehyde gas concentration.....	29
3.8 Study of the sensor performance.....	30
3.9 The precision of sensor performance.....	34
<b>CHAPTER IV RESULTS AND DISCUSSION.....</b>	<b>35</b>
4.1 Electrospun sensor morphology.....	36
4.1.1 Effects of ratio between polymer and Schiff's reagent and electrospinning process condition on morphology of the blended PEO/Schiff's reagent/Milli-Q water electrospun fiber..	36
4.1.2 Effects of ratio between polymer and Schiff's reagent and electrospinning process condition on morphology of the blended PVA/Schiff's reagent/Milli-Q water electrospun fiber..	39
4.1.2.1 Effect mass ratio.....	39
4.1.2.2 Effect of the electric field.....	41
4.1.2.3 Effect of the distance between needle and collector.....	42
4.2. Study of sensor stability.....	44
4.2.1. Stability of heat.....	44
4.2.1.1 Schiff's reagent.....	44
4.2.1.2 Film sensor.....	45
4.2.1.3 Electrospun sensor.....	46
4.2.2 Stability at room temperature.....	46
4.2.2.1 Schiff's reagent.....	47
4.2.2.2 Film sensor.....	48
4.3 Process of generating formaldehyde gas.....	49
4.3.1 Reaction time of formaldehyde and acetylacetone .....	49
4.3.2 Working time.....	50
4.3.3 Effect of temperature.....	51
4.3.4 Effect of stirring rate.....	52

	<b>Page</b>
4.4 Concentration of generated formaldehyde gas.....	53
4.4.1 Calibration curve.....	53
4.4.2 Calculated concentration of formaldehyde gas generated.....	54
4.5 Sensor performance testing.....	55
4.5.1 Electrospun sensor.....	55
4.5.2 Film sensor.....	57
4.6 Precision of sensor performance.....	60
<b>CHAPTER V CONCLUSIONS</b> .....	<b>62</b>
<b>REFERENCES</b> .....	<b>65</b>
<b>VITA</b> .....	<b>68</b>

## LIST OF TABLES

<b>Table</b>	<b>Page</b>
2.1 Physical properties of formaldehyde.....	5
3.1 The apparatus lists.....	16
3.2 Chemical list.....	18
3.3 The various weight ratio of PEO/Schiff's reagent/Milli-Q water.....	22
3.4 The various weight ratio of PVA/Schiff's reagent/Milli-Q water .....	23
4.1 Average size diameter of electrospun fibers fabricated using the electric field of 20 kV and the distance between the needle tip and the collector of 25 cm; viscosity and electrical conductivity of the blended PVA/Schiff's reagent/Milli-Q .....	40
4.2 The calculated of generated formaldehyde gas concentrations .....	54
4.3 The Absorbance at 580 nm of the electrospun and film sensor tested with pure formaldehyde gas as calculated concentration range of 120.96 - 122.64 $\mu\text{g/L}$ .....	61

## LIST OF FIGURES

Figure		Page
2.1	The structure of fuchsin dye.....	5
2.2	The structure of schiff's reagent.....	6
2.3	The mechanism of the Schiff reagent and formaldehyde.....	7
2.4	Set up of Electrospinning .....	8
2.5	Demonstration of the solution at the end of the capillary.....	9
2.6	Structure of reagent 4-Amino-4-phenylbut-3-en-2-one.....	13
2.7	Reaction between of formaldehyde and $\beta$ -diketone.....	14
3.1	Schematic of the electrospinning process.....	21
3.2	Film casting equipment.....	24
3.3	Set-up of thermal stability.....	26
3.4	The generated formaldehyde gas system.....	27
3.5	The head space bottle containing acetylacetone solution .....	28
3.6	Electrospun on metal net.....	31
3.7	Film on metal net.....	31
3.8	The generated formaldehyde gas system.....	33
3.9	The generated formaldehyde gas system.....	34
4.1	Reaction of Schiff's reagent and formaldehyde.....	35
4.2	Optical micrographs of electrospun fiber prepared from PEO / Schiff 's reagent / Milli-Q water using various mixing ratios. The electric potentials and the distances between needle and collector; a) 8:92:0 %w/w ratios 15 kV, 20 cm; b) 8:92:0 %w/w ratios, 20 kV, 20 cm; c) 9:91:0 %w/w ratios, 15 kV, 20 cm ; d) 9:91:0 %w/w ratios, 20 kV, 20 cm. All of a), b), c), and d) were spun using the flow rate of 0.2 mL/hr and spinning time was three hours.....	37

<b>Figure</b>	<b>Page</b>	
4.3	Optical micrographs of electrospun fiber fabricated at various mass ratio PEO / Schiff 's reagent / Milli-Q water, electric potentials and the distances between needle and collection screen; a) 10:80:10 %w/w ratios, 15 kV, 20 cm; b) 10:80:10 %w/w ratios, 20 kV, 20 cm; c) 10:90:0 %w/w ratios, 15 kV, 20 cm; d) 10:90:0 %w/w ratios, 20 kV, 20 cm. All of a), b), c), and d) used the same flow rate of 0.2 mL/hr. The time using in the electrospinning process was three hours.....	38
4.4	SEM micrographs of 10:90:0 weight ratio of PVA/Schiff's reagent/Milli-Q water electrospun fiber under constant flow rate of 0.1 mL/hr and the distance between needle and collector of 25 cm using following processing conditions a) 15 kV, b) 20 kV, and c) 25 kV. Original magnification of 1,000 x and inset 5,000 x.....	42
4.5	SEM micrographs of 10:90:0 weight ratio of PVA/Schiff's reagent/Milli-Q water electrospun fiber under constant flow rate of 0.1 mL/hr and electric field of 20 kV using following processing conditions a) 15 cm, b) 20 cm, and c) 25 cm. Original magnification 1,000x and inset 5,000x.....	43
4.6	The thermal stability of Schiff's reagent solution at various temperatures of 40, 50, 60, and 70 °C.....	45
4.7	The thermal stability of film at temperatures of 60 and 70 °C.....	45
4.8	The thermal stability of the electrospun fiber mats at 40, 50, 60, and 70 °C.....	46
4.9	The time stability of Schiff's solution between 1-30 days.....	47
4.10	The time stability of Schiff's solution .....	47
4.11	The time stability of film between 1-30 days.....	48
4.12	The time stability of film .....	48
4.13	Reaction of formaldehyde and acetylacetone solution.....	<b>49</b>

**Figure**

	<b>Page</b>
4.14 Reaction time between generated formaldehyde gas and acetylacetone solution.....	50
4.15 Working time of generated formaldehyde gas system.....	51
4.16 Absorbance value of generated formaldehyde gas at various temperatures.....	51
4.17 Absorbance value of generated formaldehyde gas at various stirring..	52
4.18 Calibration curve of a acetylacetone solution versus various concentration formaldehyde solutions.....	53
4.19 Images of the 10:90:0 mass ratio of PVA, Schiff's reagent and Milli-Q water electrospun fiber sensor after exposure to formaldehyde gas at concentration of blank, 61, 67, 76, 87, 102 and 122 $\mu\text{g/L}$ .....	55
4.20 The absorbance spectra of the 10:90:0 %w/w blended PVA, Schiff's reagent and Milli-Q water electrospun sensor after exposuer to formaldehyde gas at concentration of blank, 61, 67, 76, 87, 102 and 122 $\mu\text{g/L}$ .....	56
4.21 The relationship between absorbance value at 580 nm and various concentration formaldehyde: 61, 67, 76, 87, 102 and 122 $\mu\text{g/L}$ resepectively.....	57
4.22 The absorbance spectra of the 10:90:0 %w/w blended PVA, Schiff's reagent and Milli-Q water film sensor after exposuer to formaldehyde gas at concentration of blank, 61, 67, 76, 87, 102 and 122 $\mu\text{g/L}$ .....	58
4.23 The absorbance spectra of the 10:90:0 %w/w blended PVA, Schiff's reagent and Milli-Q water film sensor after exposuer to formaldehyde gas at concentration of blank, 61, 67, 76, 87, 102 and 122 $\mu\text{g/L}$ .....	58
4.24 The absorbance value at 580 nm and various concentration formaldehyde of blank, 61, 67, 76, 87, 102 and 122 $\mu\text{g/L}$ .....	59

**LIST OF ABBREVIATIONS AND SYMBOLS**

cm	Centimeter
cm <sup>2</sup>	Square centimeter
°C	Degree Celcius
K	Kelvin
kV	Kilovolt
g	Gram
mg	Milligram
mg/m <sup>3</sup>	Milligram per cubic meter
M	Molar concentration
MPa	Mega Pascal
min	Minute
mL	Milliliter
μL	Microliter
mm	Millimeter
nm	Nanometer
ppm	Part per million
ppb	Part per billion
RSD	Relative standard deviation
S/m	Siemens per meter
%w/v	Percentage weight by volume

# CHAPTER I

## INTRODUCTION

Formaldehyde is an important chemical that is widely used in construction, carpeting, textiles, wood composites, medication, and in the chemical industry. Formaldehyde can release itself from several sources to an indoor environment, such as manufacture wood product, particle board, household material, and also the furniture [1]. Formaldehyde has effects on human health. In addition, its carcinogenic and mutagenic properties cause damage to nervous system irritation to eyes and noses, and respiratory-related diseases called “sick house syndrome” [2]. The World Health Organization (WHO) has set a safe limit of exposure to formaldehyde at a maximum of 0.08 ppm ( $\text{mg}/\text{m}^3$ ) average over 30 minutes [3].

The method mostly used for detecting formaldehyde gas is an adsorption to a filter or into a liquid solution, and analyze it later with an electrochemical detection [4], ion chromatography [5], and a high performance liquid chromatography [6]. Although these methods were developed for determining a low-concentration of formaldehyde gas below *parts per billion (ppb)* levels but, these methods required an expensive instruments. Therefore, a development for a simple, inexpensive, and portable sensor was the main topic of our study.

Optical sensor is a sensor measuring changes in property of the light for detecting, such as an absorbance, fluorescence, or reflectance [7]. The optical sensor should contain a reagent that would change its color or show different light signal when exposed to the sample, this reagent called “colorimetric reagent” [8]. Most of



previous work used a colorimetric reagent for sensing a formaldehyde gas such as 4-amino-4-phenylbut-3-en-2-one [9], 4-amino-3-hydrazino-5-mercapto-triazole (AHTM) [10], and acetylacetone solution [11]. However, all of these methods require an instrument and sample pretreatment steps for determination.

Among many types of colorimetric reagent, Schiff's reagent is the one of the most selective reagent for a formaldehyde gas sensing. Schiff's reagent exposed to formaldehyde gas will change its color from yellow to violet, which can be detected by naked-eye [12]. Therefore, this Schiff's reagent was used as the colorimetric reagent for this study, and the formaldehyde gas sensor was created by both film casting and electrospinning technique. Casting method is a preparation of a thin film, which is the simplest way to produce sensor. Electrospinning method is a preparation of the polymer fiber which had many advantages such as high surface-area-to-volume ratio and high pore volume [13].

### **1.1 Research Objective**

The objective of this work is to demonstrate the potential novel optical sensor for formaldehyde gas determination by using Schiff's reagent as a colorimetric reagent in a polymer films and electrospun fibers.

### **1.2 Scope of the Research**

The scope of this research includes:

- 1) Fabrication of an optical sensor using Schiff's reagent blended with two types of polymer in various ratios by casting and electrospinning.
- 2) Characterization of the optical sensors by using Scanning Electron Microscope (SEM)
- 3) Study of the effect of various condition of fabricating process on morphology of sensor and sensor performance.
- 4) The precision of the sensor response.

### **1.3 Benefits of the research**

This research aims to obtain a portable and inexpensive optical sensor for determination of formaldehyde gas.

## CHAPTER II

### THEORY AND LITERATURE REVIEW

#### 2.1 Formaldehyde

##### 2.1.1 Properties of formaldehyde [14]

A formaldehyde molecule is an organic compound composed of one carbon atom bonded to two hydrogen atoms and double bonded to one oxygen atom. The chemical formula of formaldehyde is  $\text{CH}_2\text{O}$ . The several forms could be solid, liquid or gas.

The properties of formaldehyde are

- Colorless
- Flammable
- Soluble in water at room temperature
- Highly reactive
- Strong odor

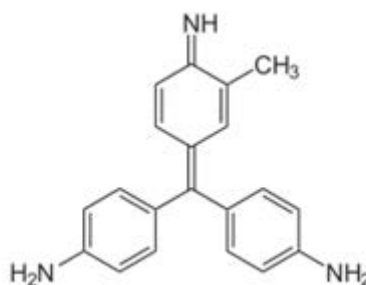
It is commonly used in liquid form as a 37-40% aqueous solution known as **formalin** and in its solid form as a fine, white powder called **paraformaldehyde**. Its physical properties are listed in Table 2.1.

**Table 2.1** Physical properties of formaldehyde [15]

Physical properties	
Molecular formula	CH <sub>2</sub> O
Molar mass	30.03 g mol <sup>-1</sup>
Appearance	Colorless gas
Density	0.8153 g/cm <sup>3</sup> (- 20 C°)
Melting point	- 92 C°, 181 K, - 134 F°
Boiling point	- 19 C°, 254 K, - 2 F°
Solubility in water	400 g dm <sup>-3</sup>

## 2.2 Schiff's reagent [16]

In early of an organic chemistry, the reaction developed by Hugo Schiff called Schiff's reagent has been used in chemical test to detect many organic aldehydes. These Schiff reagent was composed of material such as fuchsin, sodium bisulfite, and acid. The structure of the fuchsin shows in Figure 2.1

**Figure 2.1** The structure of the fuchsin.

### Mechanism of Schiff's reagent solution [17]

The color of Schiff's reagent solution appeared due to the visible wavelength absorbance of its central quinoid structure and "discolorized" upon sulfonation at its central carbon atom by sulfurous acid. The structure of the Schiff's reagent is shown in Figure 2.2.

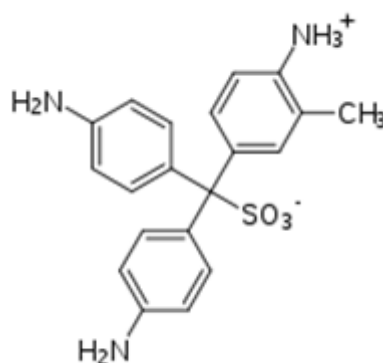


**Figure 2.2** The structure of the Schiff reagent.

The reaction of Schiff reagent with aldehydes is complicated with some researcher groups reporting many reaction products with model combined. The pararosaniline and bisulfite combined together, the currently accepted mechanism use to make the decolorized adduct with sulfonation at the central carbon as shown in Figure 2.2. Then, the uncharged aromatic amine groups react with the aldehyde being tested to form two aldimine groups (function group of imine). The carbinolamine(hemiaminal) intermediate is formed and dehydrated by the Schiff base. Then, these electrophilic aldimine groups react with bisulfite,  $\text{Ar-NH-CH(R)-SO}_3$  product, and other resonance-stabilized groups with the product, it give result as positive test with magenta color.

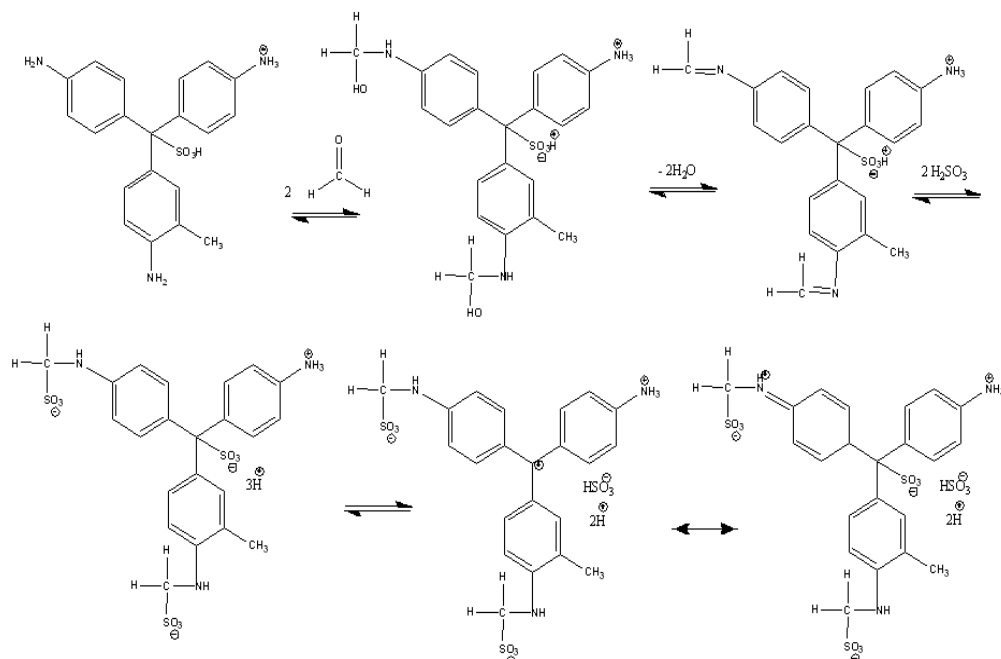


**Figure 2.3** The mechanism of the Schiff reagent and formaldehyde [18]

### 2.3 Electrospinning technique [19]

Electrospinning or electrostatic spinning was invented in 1914, but it was widely known in the 1930, as a way to overcome liquid tension and generate the elongation (jet) in the polymer of ionic solution. In the connection with a high voltage power supply resulting in elongation of the polymer solution in capillary droplet formed a line with a small overlap on the substrate (collector) which is a metal material or conductive properties. This procedure of spinning fibers can be used to prepare an extremely small fiber. The fibers size can be less than 10 nm to a several micrometers. The fibers can also be prepared in a short time. However, even if the speed of spinning is much higher, due to the size of the fiber being very small, it also takes some time to get enough amount of fiber. Because the overlapping of small

fibers, creating a material with high porosity. It can be applied in several medical benefits.

### 2.3.1 The main equipment used in the electrostatic fiber spinning [20]

Electrospinning setup consists of three main parts, as shown in Figure 2.3 .

2.3.1.1 A high voltage generator, generating voltage between the needle of the polymer solution (emitting electrode) and the supporting fibers (collecting electrode) by using the voltage in the range of 0-30 kV. Electromotive force should be in the milliamps to avoid the danger of electric shock to the operator.

2.3.1.2 The tubes containing the polymer solution may be a pipette or syringe. Syringe pump was used for controlling the flow rate of the polymer solution.

2.3.1.3 A fiber collector.

It may have a different characteristic such as the metal grill, metallic rotating drum, a roller covered with metal, aluminum foil.

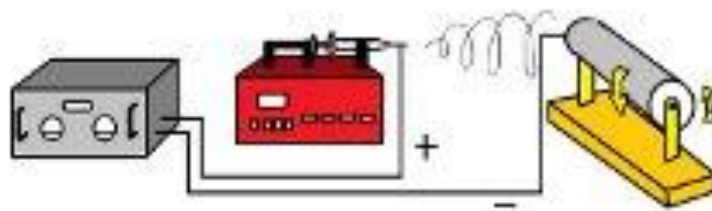
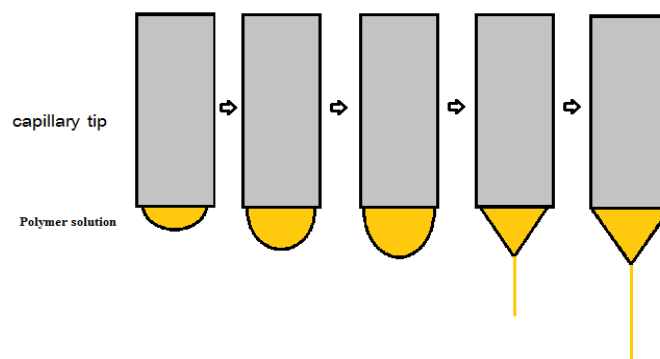


Figure 2.4 Electrospinning setup

### 2.3.2 Principles of spinning fibers. [21]

The production of polymer fibers in nanometer scale is called electrostatic spinning or electrospinning. The polymer solution was received a high electric potential, the polymer solution will elongation (jet) from the capillary and then the solvent evaporation occurs before the polymer solution moves into the collector. The small molten polymer disorganized into a collector by connecting an electrode to a polymer solution, and another electrode connected to the collector (most of the collector is connected to the ground wire). When an electrical charge goes into the polymer solution, an ion will move to the surface of the solution at the edge of its capillary, as the electric field strength increases. The solution changes its shape from a sphere into a cone (also known as the Taylor cone). When the electric field is increased to a point where the electric force is greater than the surface tension of the liquid, the polymer solution will eject from the edge of the capillary and will become unstable. Then the polymer solution will elongate (jet) and decrease in diameter and the solvent will evaporate, leaving only a polymer fiber as shown in Figure 2.4



**Figure 2.5** Demonstration of the solution at the end of the capillary



### **2.3.3 Mechanism of the fiber [22]**

Electrospinning techniques procedures have three steps as follows.

#### **2.3.3.1 Initiation of charged jet**

At the beginning, because of the voltage between the needle and collector, the polymer solution moves to the tip of the needle. As the voltage increases, it will increase the accumulation of the charge (it may be negative pole depending on the power source) at the surface of the solution. The electrical repulsion between the charges will result in a drop of water shape to a cone, called Taylor cone. When the repulsion between the charges on the surface of the solution becomes higher than the surface tension, the solution will elongate (jet) from the top of the Taylor cone.

#### **2.3.3.2 Elongation of charged jet**

The polymer solution was ejected and landed on the collector, an elongation of the polymer solution was continuously rotated in one direction and unstable. Various distances between the tip of the needle and the collector will result in different fiber diameter. AS the distance increases, the fiber diameter will be smaller and then it will bend due to the electrical repulsion (Electrically driven bending instability) of the charge on the fibers.

#### **2.3.3.3 Solidification of the charged jet**

During the elongation of the solution, the solvent evaporated, making the polymer solution solidity into the fiber. Evaporation of the solvent may occur before or after the polymer solution lands on the collector.

In procedures and processes that fabricate fibers, It seems that the elongation of the polymer solution is a key factor in making a smaller fiber. But there are still other factors that affect as well, such as the splitting of two or more polymer solutions, depending on the type of polymer and variables in the production process.

### **2.3.4 Factors influencing the fiber spinning [23]**

#### **2.3.4.1 solution factor**

The solution properties including viscosity of the solution, electrical conductivity, surface tension, molecular weight of the polymer, solubility system, and the temperature of the solution are parameters affecting the electrospinning process. As the viscosity of the solution and the molecular weight increases, the diameter of the fiber will be larger. However, the electrical conductivity and temperature of the solution increases, the fibers will also reduce in size. However, these factors may not be in accordance with the above case due to the affect by other factors.

#### **2.3.4.2 Factor of processing.**

This factor was composed of the voltage, the distance between of the needle to the collector (gap distance), flow rate of polymer solution, the size of the needle injection (spinneret size). If the voltage distance between the needle tip at the collector is increased, it will result in a smaller fiber. However, the increase in the flow rate of the polymer solution and the size of the needle injection will make the fibers larger.

### **2.3.5 Properties of nanofibers.**

The shape of the produced fibers are sometimes shaped like beads, porous or sometimes oddly shaped fibers. The shape and size of the fibers are dependent on the type of polymer, properties of the solvent, and the conditions of production.

### **2.4 Casting technique**

The film casting technique is used to produce thin film. The process was prepared by pouring the studied polymer solution in to plastic box. The polymer later became thin film by evaporation of its solvent. During a casting process, the thickness of the film can be control by manipulate the weight of the polymer and evaporation rate of solvent.

### **2.5 Literature review**

In this work, the developed formaldehyde gas sensor using the naked-eye for analysis will change its color after being exposed to formaldehyde gas.

In 2003, Suzuki [9] studied the detection of formaldehyde gas from elements created by cellulose filter paper. They include 2 different types of reagents, [4-Amino-4-phenylbut-3-en-2-one] and [3-Amino-1, 3-diphenyl-prop-2-en-1-one] respectively, shown in Figure 2.5. When both sensors exposed with formaldehyde gas, it changed color from colorless to yellow. Limit of detection (LOD) is low (0.05

ppm HCHO). In addition, comparing both reagents found 4-Amino-4-phenylbut-3-en-2-one has a higher sensitivity.

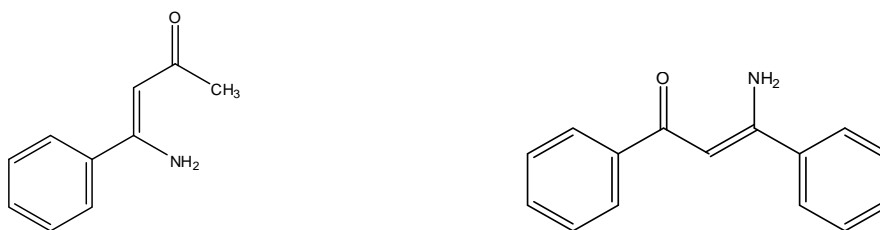


**Figure 2.6** a) 4-Amino-4-phenylbut-3-en-2-one b) 3-Amino-1, 3-diphenylprop-2-en-1-one

In 2005, Kawamura [10] had developed a novel hand-held HCHO gas sensor for the sick building syndrome (SBS) by glass filter and silica filter, containing [4-amino hydrazine-5-mercapto-1, 2, 4-triazole (AHMT)] blending with [potassium hydroxide (KOH)]. AHMT reagent on the filter reacted with HCHO to produce a change in its color. The limit of detection (LOD) of 0.04 ppm HCHO within a sampling time of 3 minutes was achieved.

In 2008, Maruo [11] had developed a sensor element for detecting formaldehyde gas. This sensor element was made from a porous glass impregnated with both a Schiff's reagent and an acid. When the sensor was exposed with formaldehyde its color changed from yellow to violet and it will become darker if the concentration of the formaldehyde gas increases. LOD of 10 ppb HCHO and absorbance appeared at 580 nm.

In 2008, Maruo [12] had developed a sensor element for detecting formaldehyde gas by using reaction  $\beta$  – diketones, three different reagents with formaldehyde gas, shown in Figure 2.6. Each sensor was made from a porous glass impregnated with three reagents : acetylacetone, 1-phenyl- 1,3-buta-nedionec and

1,3-diphenyl-1,3-propanedione, respectively. In this work the sensor made from acetylacetone reagent was the best detector, after the sensor exposure formaldehyde its changed color. LOD 14 ppb HCHO and absorbance appeared at 407 nm.

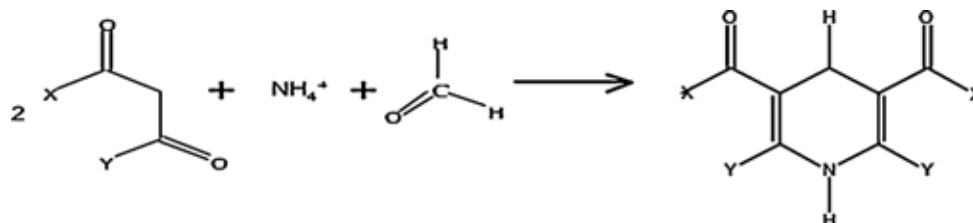


**Figure. 2.7** Reaction between formaldehyde gas and β – diketones, acetylacetone : X =CH<sub>3</sub>, Y= CH<sub>3</sub>, 1-phenyl- 1,3-butanedione : X= C<sub>6</sub>H<sub>5</sub>, Y= CH<sub>3</sub> and 1,3-diphenyl-1,3-propanedione: X= C<sub>6</sub>H<sub>5</sub>, Y= C<sub>6</sub>H<sub>5</sub>

In 2010, Bunkoed [24] developed a selectivity sensor for detecting formaldehyde gas. The sensor made from sol-gel and using reaction β – diketones with formaldehyde gas and then detected formaldehyde gas, changed its color from colorless to yellow. In addition, the sol-gel sensor from acetylacetone reagent was the best detector because of the sensor was more selective and sensitive than the sensor from methyl acetoacetate reagent. The limit of detection (LOD) is 0.03 ppm HCHO

In 2011, Zhang [25] studied how to determine formaldehyde gas by electrospun fibers. This work used the electrospinning process, polystyrene(PS) fibers were electrospun and deposited on quartz crystal microbalance (QCM), and followed by dropping polyethyleneimine (PEI) solution onto fibrous PS membranes. The sensor had a high surface to volume (47.25 m<sup>2</sup> /g) and high porosity. The limit of detection (LOD) was 3 ppm HCHO, but this sensor could not be seen by the naked-eye for analysis.

In this work, the developed formaldehyde gas sensor was created by electrospinning and film casting technique using Schiff's reagent. These sensors will change its color after being exposed to a formaldehyde gas it can be analyze by the naked-eye.

## CHAPTER III

### EXPERIMENTAL

#### 3.1 Apparatus

The apparatus used in this study are listed in Table 3.1.

**Table 3.1** Apparatus lists

Apparatus	Company, model	Purpose
1. Scanning electron microscope (SEM)	JEDL, model JSM-5410LV Japan	Morphology characterization
2. UV-visible spectrophotometer	Hewlett Packard 8453 Perkin-Elmer: Pyris 1	Record spectra and absorbance measurements
3. Conductivity/TDS/0C/F meter	Eutech instruments, model CON 510	Conductivity measurements
4. Programmable Viscosity	Brookfield, model DV-II	Viscosity measurements
5. High voltage power supply	Spellman CZE 1000R	Electrospinning set-up
6. Syringe pump	QIS, model NE1000	Electrospinning set-up

<b>Apparatus</b>	<b>Company, model</b>	<b>Purpose</b>
7. Fiber-optic spec trophotometer	Ocean optic red tide USB 650	Record spectra and reflectance measurements
8. Magnetic stirrer with heating hot plate	Model C-MAG HS 10 digital, IKAMAG	Temperature and stirring rate controller
9. Flow meter	Model RMA, Dwyer	Flow rate controller
10. Head space bottle with bottle cap	Vertical	Generating gas system
11. Stainless steel ball valve ½ inch	J.S. salakpan	Air gate
12. 500 mL-triple necks round bottom flask, borosilicate glass grade.	N.K. supply laboratory	Sensing chamber
13. 500 mL glass flask, borosilicate glass grade.	N.K. supply laboratory	Generating gas system
14. Teflon tube diameter of 8 mm.	N.K. supply laboratory	Generating gas system
15. T-way junction	J.S. salakpan	Generating gas system



16. Temperature controller	IKA, EST-D5	Controlling temperature of hot bath
17. Reflectance probe	Ocean optics	Reflectance measurements
18. Lamp	HI- TEK, Halogen 12V 50W	Light source of Fiber-optic spectrophotometer
19. Micropipette	Eppendorf Research plus	Pipette solution

---

### 3.2 Chemicals

All chemicals used for sensor preparation were purchased in analytical grade from suppliers listed in Table 3.2

**Table 3.2** Chemicals list

Chemicals	Supplier
Polyvinyl alcohol, PVA. High molecular weight (Mw 146,000-186,000)	Sigma Aldrich
Polyethylene oxide , PEO (Mw 400,000)	Sigma Aldrich
Formaldehyde solution	Sigma Aldrich

Basic Fuchsin, Pure, Certified	Acros organic
Sodium sulfite	Ajax Finechem
Hydrochloric acid	Fisher scientific
Phosphoric acid	Merck
Acetyl acetone	Carlo Erba
Ammonium acetate	Fisher scientific
Acetic acid	Fisher scientific
Nitrogen gas 99.99%	Praxair

---

### 3.2.1 Preparation of reagents

#### 3.2.1.1 Schiff's reagent solution

Schiff's reagent solution is prepared by mixing 0.1 g of fuchsin, 1.0 g of sodium sulfite, and 1.0 mL of HCl in 100 mL of Milli-Q water. Then the Schiff's reagent was mixed with 100 mL and 20 mL of phosphoric acid.

#### 3.2.1.2 The mixture of polymer media/ Schiff's reagent/ Milli-Q water solution

The polymer solution containing a polymer (PEO or PVA), Schiff's reagent, and Milli-Q water were prepared by weighing each component and then mixed in a glass bottle. The solution was stirred for 8 hours, before using in electrospinning or casting process. The detail of polymer solution preparation was shown in Table 3.3 and 3.4

### **3.2.1.3 0.8% v/v of acetylacetone solution**

The 100.00 mL-acetylacetone solution was prepared by dissolving 0.8 mL of acetylacetone solution, 8.0 mL of acetic acid, and 30.00- 30.50 g of ammonium acetate. All of liquid was drawn by using micropipette. All of the component mentions above were mixed with Milli-Q water in 100.00 mL-volumetric flask.

### **3.2.1.4 Formaldehyde standard solutions**

A 1000 ppm formaldehyde solution was prepared by mixing the 2.70 mL of 37 %w/v formaldehyde solution to 1 L with Milli-Q water using volumetric flask. Before diluting it with Milli-Q water in the formaldehyde solution with concentrations of 50, 100, 200, 500, 1000, 1500, and 2000  $\mu\text{g/L}$  were prepared by pipetting the appropriate volume of 1000 ppm and mixing in volumetric flask. This formaldehyde standard solution was used to construct constructed a standard curve.

## **3.3 Sensor fabrication**

### **3.3.1 Electrospinning process**

In this study, a basic apparatus composed of a high voltage power supply, a syringe pump and a metal net on rotating collector was set up for electrospinning processing. The experiment set-up is shown in Figure.3.1. A polymer solution was put into a 3 mL plastic syringe with a blunt needle tip of 0.8 mm in diameter. The flow rate of the solution was controlled using syringe pump. The electrospun fibers were collected on either aluminium foil or metal net attached on the aluminum foil wrapping around the rotator. The experiments were processed at room temperature.

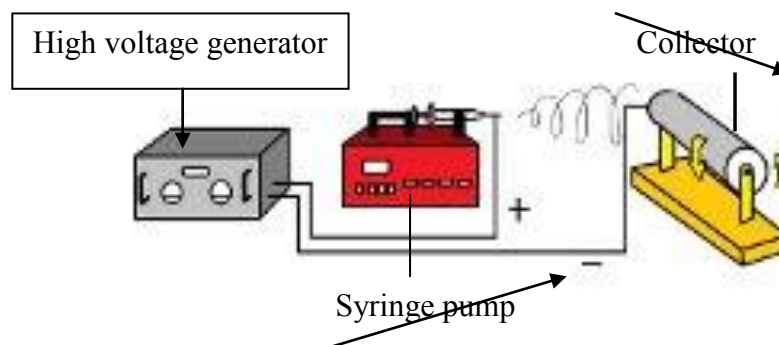


**Figure 3.1** Schematic of the electrospinning process.

### **3.3.1.1 Effect of the weight ratio of PEO/ Schiff's reagent/ Milli-Q water on the morphology of electrospun fibers**

The various weight ratios of the PEO/ Schiff's reagent/ Milli-Q water were used to determine the effect on morphology of the electrospun fibers. The preparation details of blended PEO/ Schiff's reagent/ Milli-Q water was shown in Table 3.3.

Condition of electrospinning process using are the distance between needle to aluminium foil on the collector of 20 cm, the electrical potential 15-20 kV, and flow rate controlled to 0.2 mL/rh. The time using in the electrospinning process was three hours.

**Table 3.3** The various weight ratios of PEO/ Schiff's reagent/ Milli-Q water in solution

Ratios of PEO: Schiff's reagent: MilliQ-water (%w/w)	Weight (g)		
	PVA	Schiff's reagent	MilliQ-water
8 :92:0	0.80-0.83	9.20-9.23	-
9 :91:0	0.90-0.93	9.10-9.13	-
10:90:0	1.00-1.03	9.00-9.03	-
10:80:10	1.00-1.03	8.00-8.03	10.00-10.03

### 3.3.1.2 Effect of the weight ratio of PVA/Schiff's reagent/Milli-Q water on the morphology of electrospun fibers

The various weight ratios of the PVA/ Schiff's reagent/ Milli-Q water were used to determine the effect on morphology of the electrospun fibers. The preparation details of blended PVA/ Schiff's reagent/ Milli-Q water shown in Table 3.4.

Condition of electrospinning process were the distance between needle to metal on the collector of 15-25 cm, the electrical potential 15-25 kV, and flow controlled to 0.1 mL/hr. General, the spinning time is ...hours. However, for sensor performance study, the time using in the electrospinning process was twenty hours.

**Table 3.4** The various weight ratios of PVA/ Schiff's reagent/ Milli-Q water in solution

Ratios of PVA: Schiff's reagent: MilliQ-water (%w/w)	Weight (g)		
	PVA	Schiff's reagent	MilliQ-water
10:90:0	1.00-1.03	9.00-9.03	-
10:80:10	1.00-1.03	8.00-8.03	1.00-1.03
10:70:20	1.00-1.03	7.00-7.03	2.00-2.03

The obtained electrospun fibers were kept in a desiccator at room temperature before performing SEM analysis.

### 3.3.1.3 Optimization of the parameters of the electrospinning process.

The effects of electric fields of 15, 20 and 25 kV were investigated in this study. The distances between the needle tip and metal net or aluminum foil on the collector were also varied between 15 cm and 20 cm.

### 3.3.2 Casting process

Based on observed results from the section 3.3.1, the polymer concentration delivering the best fiber was chosen to study in this section. A 4 mL-of the freshly polymer solution was poured into the plastic box (5x3 cm<sup>2</sup>), as shown in Figure 3.2 and kept it in the hood at room temperature for 48 hour. All films were kept for 3-7 days in the desiccators for later usage.



**Figure 3.2** Film casting equipment

## 3.4 Characterization

### 3.4.1 Solution viscosity

A freshly prepared polymer solution was measured 3 times by a viscometer.

### **3.4.2 Solution conductivity**

A freshly prepared polymer solution was measured 3 times by a conductivity meter.

### **3.4.3 Morphology of electrospun fibers.**

Scanning Electron Microscope (SEM) with an accelerating voltage of 15 kV was used to investigate the morphology and size of the electrospun fibers. All of the samples were sputter-coated with gold prior to SEM observation. An average diameter ( $\pm$ SD) of random 100 fibers was calculated by Semfore program.

## **3.5 Study of sensor stability**

In this study, the stability or fault positive of three different types substrates containing same Schiff's reagent: Schiff's reagent solution, film sensor, and electrospun sensor toward heat and storage time was evaluated. In this study, 7.00 mL of the Schiff's reagent solution, the film size of 2x2 cm<sup>2</sup>, and electrospun on metal size of 12x12 mm<sup>2</sup> were us

### **3.5.1 Thermal stability**

The studied substrates were kept in the hot bath of which temperature was kept constantly at 40, 50, 60, or 70 °C for 1-12 hour as shown in Figure 3.3. Finally the absorbance at 580 nm was monitored for every hour for all substrates. The UV-visible spectrophotometer was employed for Schiff's reagent solution and film whereas the Optic-fiber spectrophotometer was used for electrospun fiber.



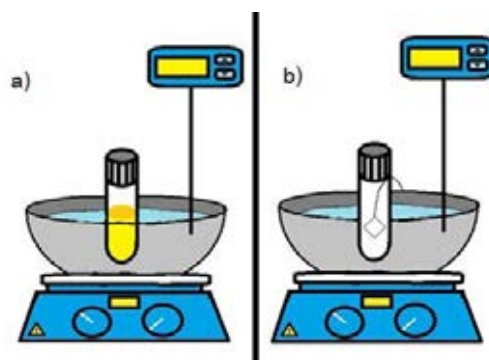


**Figure 3.3** Set-up of a) Schiff's reagent solution, b) film and electrospun fiber

### 3.5.2 Time stability

Film and Schiff's reagent were kept uncovered at room temperature between 26-28 °C for 1-30 days. Finally, the sensor was analyzed by using the UV-visible spectrophotometer at 580 nm.

### 3.6 Process of generating formaldehyde gas

Formaldehyde gas was generated by heating and stirring a 200 mL of 37 % w/v formaldehyde solution (formalin) in gas generator flask combining with bubbling nitrogen gas at the flow rate of 100 mL/min into this solution for whole time. The set-up of formaldehyde gas generating system is shown in Figure 3.4. The apparatus for using set-up of formaldehyde gas generating system are shown in Table 3.1.

First, the valve number one was on to bubble into formaldehyde solution and let it flows to to the waste using period of time obtained from section 3.6.2. Waste was created from Schiff's reagent for entrap generated formaldehyde gas for wait the generated gas to be equilibrium. After generated formaldehyde gas reached its equilibrium time then valve number one was turned off and valve number two was

turned on. Then the generated formaldehyde gas was flown to either 7mL of acetylacetone solution for determination the concentration of generated formaldehyde gas and b) sensing chamber, which further describe its detail in section 3.8.

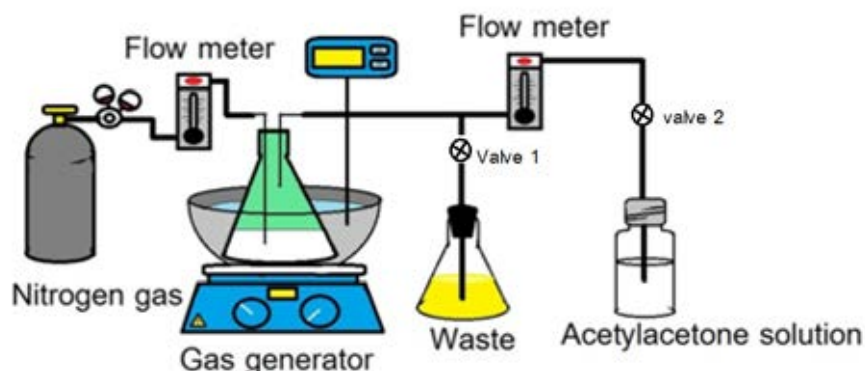


**Figure 3.4** Formaldehyde gas generating system

### 3.6.1 Reaction time

The concentration of formaldehyde gas in the gas stream was determined based on the reaction between formaldehyde gas with acetylacetone solution. Therefore, the 100 mL of generated formaldehyde gas was flown into a 7.00 mL of acetylacetone solution in slightly opened screw cap of the head space bottle for 1 minute, the head space bottle was completely sealed with bottle cap as shown in Figure 3.5. The absorbance was measured by using UV-visible spectrophotometer at 412 nm. The absorbances of products were recorded at 0, 5, 10, 15, 20, 30, 40, 50, and 60 min. The experiments were performed in triplicate.



**Figure. 3.5** The head space bottle containing acetylacetone solution

### 3.6.2 Working time

In our system, the formaldehyde gas was generated by bubbling nitrogen gas combining with heating and stirring the formalin solution. The content of formaldehyde gas in the atmosphere above the flask depends on the generating time. Therefore, the required generating time for the content of formaldehyde gas to reach equilibrium in the atmosphere and the working time range before the decrease of the formaldehyde gas content were studied. First, the nitrogen gas (flow rate 100mL/min) was flown into the generating chamber for 1 minute. The second step is turn on the valve number two to flow the generated gas into the 7 mL of acetylacetone solution in the head space bottle for 1 minute. Then the step one and two were repeated for each head space bottle until 80 minute as shown in Figure 3.4. The temperature and stirring rate of formaldehyde solution in generating flask were controlled by information obtained from section 3.6.3 and 3.6.4 respectively. The head space bottles were kept at room temperature for 20-60 minutes before measuring the absorbance at 412 nm. The optimum working time was used for future experiment.

### **3.6.3 Effect of temperature**

The effect of temperature on the quantity of generated formaldehyde gas was studied by controlling the temperature formalin solution at various temperatures at 30, 40, or 50 °C and the stirring rate was kept constant at 100 rpm.

The content of formaldehyde gas was evaluated as describe below. After the suitable working time found in section 3.6.2 was reached, the generated gas was flown into a head space bottle containing a 7.00 mL of acetylacetone solution for 1 minute. Then, the head space bottle was completely sealed with bottle cap as shown in Figure 3.5. The absorbance was measured by using UV-visible spectrophotometer at 412 nm. The experiments were performed in triplicate.

### **3.6.4 Effect of stirring rate**

The effect of stirring rate on the formaldehyde gas generation was studied at 0, 100, 380, 660, and 940 rpm. The temperature was controlled at 50 °C and the experiments were performed in triplicate.

The content of formaldehyde gas was determined as described in the section 3.7

## **3.7 Determination of generated formaldehyde gas concentration**

The concentration of generated formaldehyde gas was determined. The working steps were detailed below.

a. The calibration curve was constructed using absorbance of mixed solution and concentration of formaldehyde solution. The various concentration of formalin prepared in section 3.2.1.4 was mixed with 0.8% v/v of acetylacetone solution. Then,

the 0.50 mL of mixed solution were diluted with 3.50 mL of Milli-Q water and kept at room temperature for 20 minutes before performing the absorbance measurement at 412 nm using UV-visible spectrophotometer. The experiments were performed in triplicate.

b The formaldehyde gas was generated using the best condition found in section 3.6. The concentration of formaldehyde gas was determined by flowing 100 mL of the generated gas into 7.00 mL of 0.8% w/v acetylacetone solution in the head space bottle. The head space bottles containing acetylacetone solution and generated gas were completely sealed with bottle cap and kept at room temperature for 20 minutes. Finally, the absorbance of mixture at 412 nm was analyzed by using the UV-visible spectrophotometer. The experiments were performed in triplicate.

c The concentration of formaldehyde gas (x) was calculated using the absorbance obtained in b) and the linear equation ( $y = mx + c$ ) of the calibration curve in a), where y is the absorbance value obtained in mixed solution, x is the concentration of formaldehyde solution.

The detail of calculation process will be shown in section 4.4.2

### **3.8 Study of the sensor performance**

In order to study the sensor performance, electrospun sensor was fabricated on the metal net as shown in Figure 3.6 (a). Then, the sensor was cut into 1 x 3 frames as shown in Figure 3.6 (b). The dimension of one frame is 12x12 mm. For the film sensor, polymer solution was casted on plastic box shown in Figure 3.7 (a) and let it air dried. Then, the polymer was stretched and attached with the metal net as shown in

Figure 3.7 (b). In each experiment, a 3-frame sensor was tested and two types of the studied sensor (electrospun fiber, film) were placed in the sensing chamber.

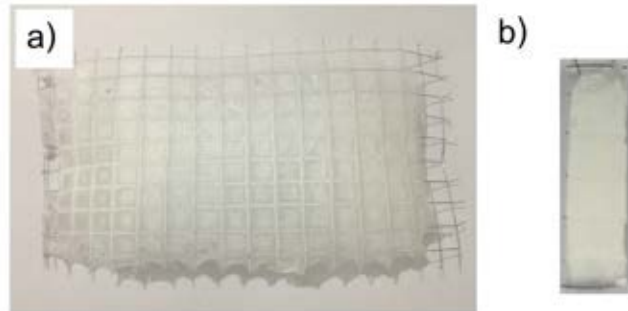


**Figure. 3.6** a) Original electrospun on metal net, b) cut three frame metal net



**Figure. 3.7** a) film on plastic box, b) film attached with metal net

The gas sensor testing system (as shown in Figure 3.8) was used to study the sensor performance. The process of testing sensor performance was shown in following steps.

a) The sensing chamber carrying the sensor inside was vacuumed using vacuum pump by turning on valve number four and number six and closed the other valves.

b) The nitrogen gas stream was divided in two ways using T-way junction connected to the flow meter one and flow meter two. Flow meter one was used to control the flow rate of the nitrogen gas, which flow into the generating flask. The flow rate was kept constant at 100 mL/min. The flow meter two was used to adjust the flow rate of the nitrogen gas, which served as the solvent to dilute the content of formaldehyde gas in the gas stream. The flow rate was controlled at 0, 20, 40, 60, and 100 mL/min

c) The generated gas and nitrogen gas from flow meter one and flow meter two were both mixed at T- way junction and flown to the waste one for 15 minutes by turn on only valve number one.

d) The generated gas was flown through the sensing chamber and flow to the waste two for 15 minutes by turning on valve number two, three, four, and five and turning valve number one

e) After 15 minutes passed, the valve number three and four were turned off. Then, the sensing flask was sealed with parafilm and kept at room temperature in normal environment for 24 hours.

f) The changing color of sensor was observed by visual detection parallel with the fiber-optic spectrophotometer detection. The fiber-optic spectrophotometer

detection was measured under dark condition by using black box to minimize any interference from the ambient light. The reflectance probe was placed 2.0 mm. above the sample. Absorption spectra of the sensor were collected at 580 nm. The responses of a sensor were collected three times at three different frames on each sensor.

The mixing ratio (mL/min) of generated formaldehyde gas and nitrogen gas in step b) were controlled by adjusting the flow rate of nitrogen gas at the flow meter number 2. The mixing ratio are 100:100 (50% HCHO), 100:80 (55% HCHO), 100:60 (62% HCHO), 100:40 (71% HCHO), 100:20 (83% HCHO) and 100:0 (100% HCHO).

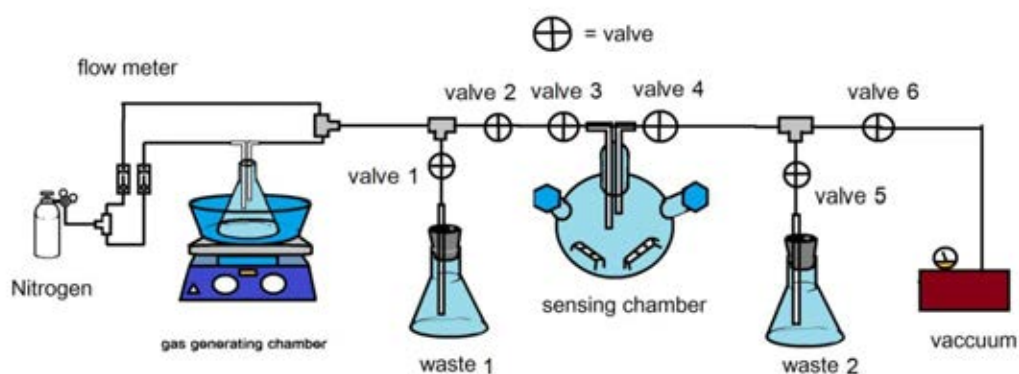


**Figure. 3.8** The generated formaldehyde gas system





**Figure3.9** The generated formaldehyde gas system

### **3.9 The precision of sensor performance**

The precision of sensor performance were evaluated on both electrospun and film sensors. The precision of sensor performance was tested three different days using one sample per day and each sample contains 3 frames. The precision of sensor performance was studied using only generated formaldehyde gas without any dilution. The testing system was set up as explained in section 3.8. After the sensors were exposed to the generated formaldehyde gas for 24 hours, the absorbance at 580 nm was analyzed using the Fiber-optic spectrophotometer. The relative standard deviation (RSD) of the absorbance at 580 nm of both electrospun sensor and film sensor was calculated.

## CHAPTER IV

### RESULTS AND DISCUSSION

In this study, the colorimetric sensors for formaldehyde gas determination were developed by blending polymer polyethylene oxide (PEO) and polyvinyl alcohol (PVA), with Schiff's reagent. After the Schiff's reagent exposed to formaldehyde, its color changed from yellow to violet, which were detected using UV-visible spectrophotometer at 580 nm. The reaction between Schiff's reagent and formaldehyde is shown in Figure 4.1. Two types of studied polymer sensors: polyethylene oxide, PEO and polyvinyl alcohol, PVA were fabricated using two different processes: electrospinning and casting methods.

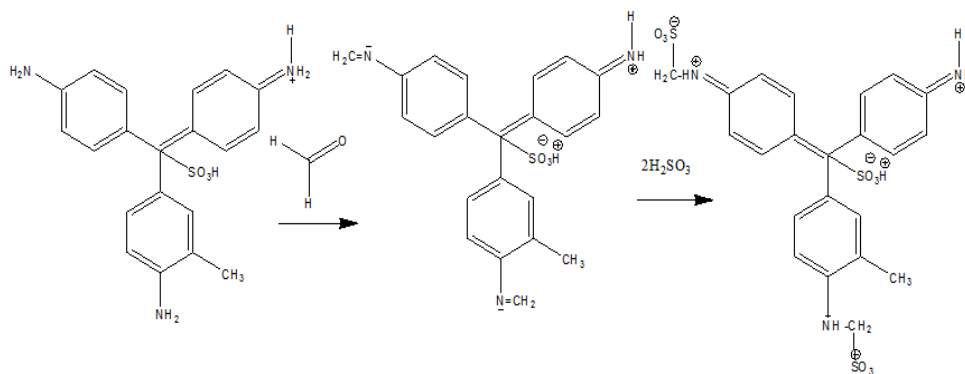


**Figure 4.1** Reaction of Schiff's reagent and formaldehyde. [18]

## **4.1 Electrospun sensor morphology**

The morphology and diameter of electrospun fibers depends on various parameters such as type of polymer, concentration of polymer solution, and other processing parameter electrospinning process [26]. The main purpose of this section was to determine a compatibility between Schiff's reagent and two carrier polymers, i.e PEO and PVA, and fiber formation ability of these mixture via electrospinning process. These two polymers shares similar properties: hydrophilicity and non-toxic [27] and abilities to dissolve in Schiff's reagent solution and it could simply be fabricated into fiber by electrospinning process.

### **4.1.1 Effects of mass ratio between polymer and Schiff's reagent and electrospinning process condition on morphology of the blended PEO/Schiff's reagent/Milli-Q water electrospun fiber**

In this part, the mixed solutions were prepared at 8:92:0, 9:91:0, 10:80:10, and 10:90:0 weight ratio of PEO, Schiff's reagent and Milli-Q water. Relatively, variation of the electric fields and the distances between the needle and the collector was also investigated. Finally, the data was analyzed with the optical microscope (OM) as shown in Figure.4.2, and Figure 4.3.

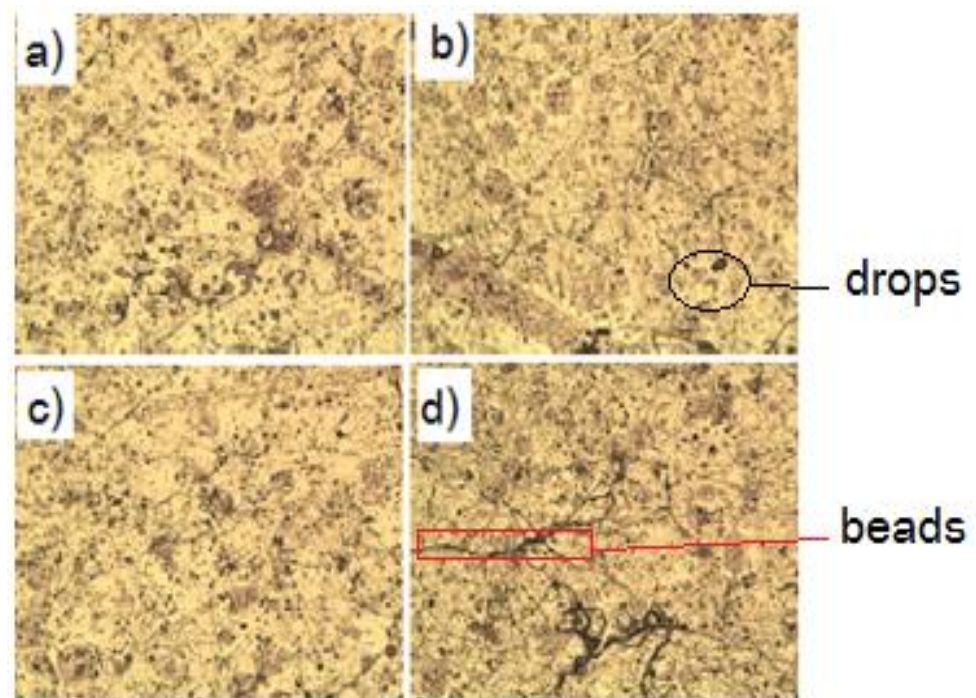


**Figure 4.2** Optical micrographs of electrospun fiber prepared from PEO / Schiff's reagent / Milli-Q water using various mixing ratios. The electric potentials and the distances between needle and collector; a) 8:92:0 %w/w ratios 15 kV, 20 cm; b) 8:92:0 %w/w ratios, 20 kV, 20 cm; c) 9:91:0 %w/w ratios, 15 kV, 20 cm ; d) 9:91:0 %w/w ratios, 20 kV, 20 cm. All of a), b), c), and d) were spun using the flow rate of 0.2 mL/hr and spinning time was three hours.

From the result of optical micrographs of the electrospun fiber mats in Figure 4.2, the 8:92:0 and 9:91:0 weight ratios, it shows a lot of drops and beads and the amount of fibers seem to be low in quantity. After the concentration of PEO was increased to 10% w/w, it also found that the electrospun sensor still have a lot of drops and beads, therefore the electrospun fiber was disqualify as shown in Figure 4.3.

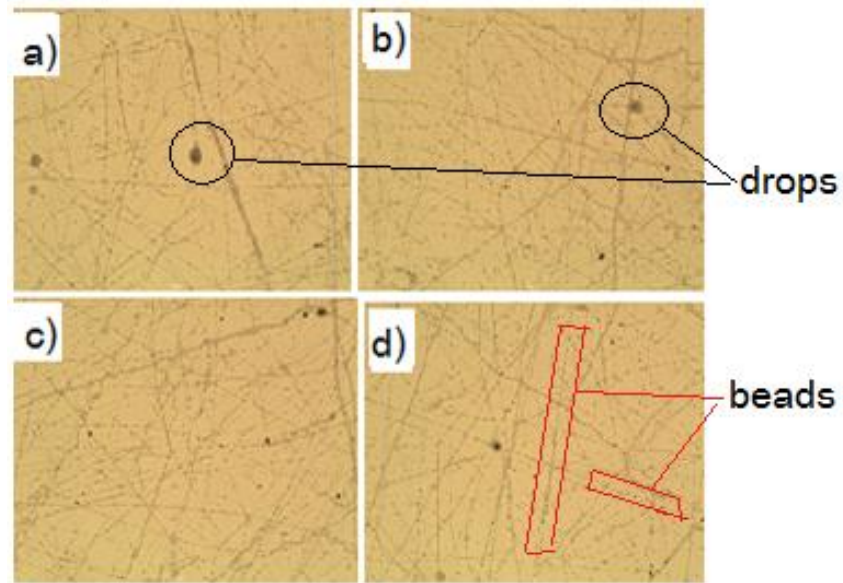


**Figure 4.3** Optical micrographs of electrospun fiber fabricated at various mass ratio PEO / Schiff's reagent / Milli-Q water, electric potentials and the distances between needle and collection screen; a) 10:80:10 %w/w ratios, 15 kV, 20 cm; b) 10:80:10 %w/w ratios, 20 kV, 20 cm; c) 10:90:0 %w/w ratios, 15 kV, 20 cm; d) 10:90:0 %w/w ratios, 20 kV, 20 cm. All of a), b), c), and d) used the same flow rate of 0.2 mL/hr. The time using in the electrospinning process was three hours.

From the result shown above, the blended PEO/Schiff's reagent/Milli-Q water is not a suitable sensor in this experiment as it has a very small amount quantity of the result of the fibers acquired, the fibers were beads and a lot of drop shown too.

#### **4.1.2 Effects of mass ratio between polymer and Schiff's reagent and electrospinning process condition on morphology of the blended PVA/Schiff's reagent/Milli-Q water electrospun fiber**

In this section, the potential of PVA as the electrospun sensor media was investigated. The studied parameters were mass ratios, electric field and the distance between needle and roller.

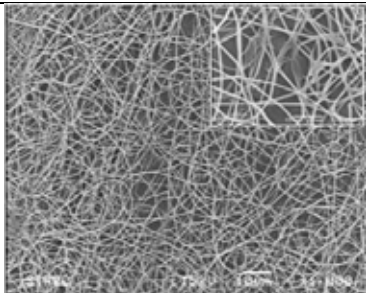
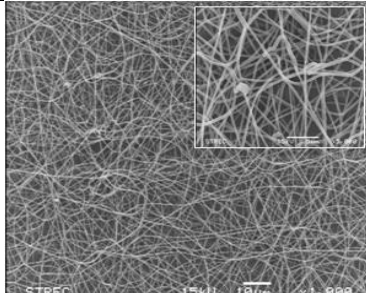
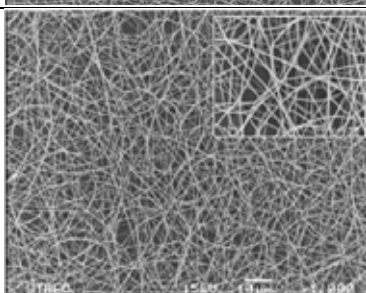
##### **4.1.2.1 Effect of mass ratio**

In this study, the various mass ratios of the blended PVA/Schiff's reagent/Milli-Q water affecting the differences of viscosities and conductivities of the polymer solution was evaluated. Viscosities and conductivities of the blended PVA/Schiff's reagent/ Milli-Q water solutions at various concentrations resulted in a difference in morphological and size of the fibers. These fibers obtained by electrospinning at electric field of 20 kV and the distance between the needle tip and the collector of 25 cm were summarized in Table 4.1.

The increase in the viscosity of the solution as the mixing ratio of Schiff's reagent increased was observed. This indicated that entanglement among PVA polymer molecules in the mixture was increased. It suggested that components in Schiff's reagent affected the interaction between PVA polymer molecules and the solvent, which could be regarded as a dilute Schiff's reagent, in a way that it increased the radius of gyration of PVA molecules. Since the conductivity of the solution depends on number of charges or ions, and their mobility; increasing in viscosity would then hinder charges mobility, and hence, solution conductivity as found here. The result in Table 4.1 showed that the 10:90:0 % w/w of PVA: Schiff's

reagent: Milli-Q water solution delivered the smallest diameter of fibers because of the highest viscosity and lowest conductivity.

**Table 4.1** Average size diameter of electrospun fibers fabricated using the electric field of 20 kV and the distance between the needle tip and the collector of 25 cm; viscosity and electrical conductivity of the blended PVA/Schiff's reagent/Milli-Q water

<b>Ratios of PVA: Schiff's reagent Milli-Q water (%w/w)</b>	<b>SEM micrographs of electrospun fiber (1000x, inset 5000x)</b>	<b>Electrical conductivity (<math>\times 10^3</math> S)</b>	<b>Viscosity (cP)</b>	<b>Average diameter of fibers (nm) (n=100)</b>
10:70:20		126.3 $\pm$ 7	3251 $\pm$ 29	393 $\pm$ 102
10:80:10		114.6 $\pm$ 12	4512 $\pm$ 35	359 $\pm$ 94
10:90:0		105.4 $\pm$ 7	5426 $\pm$ 48	342 $\pm$ 41

#### 4.1.2.2 Effect of the electric field

From our result in the section 4.1.2.1, the solution of PVA/Schiff's reagent/Milli-Q water was prepared with the ratio of 10/90/0 % w/w for the study in this section. The distance between needle tip, collector and the flow rate were kept constant but the electric potentials was studied in three values: 15 kV, 20 kV, and 25 kV. The data was shown in Figure 4.4.

Theoretically, increasing the electrical potential of the electrospinning process affects a mass transfer rate of the polymer solution from the needle to the collector causing the polymer to move from the needle to the collector a lot faster resulting in the decreasing of the fiber diameter [28]. It was found that the electric potential at 25 kV was not suitable for electrospinning process as the solvent and acid in the polymer solution did not fully evaporate in time before touching the collector [29], resulting in an unstable size and diameter fiber as shown in Figure 4.4 c.

Under a constant flow rate of 0.1 mL/hr and the distance between needle and collector of 25 cm, the fiber spun using the electric field of 15 kV (Figure 4.4 a) was not suitable comparing to electrospun fiber preparing with electric field of 20 kV in Figure 4.4 (b). The result of diameter and size of the fiber obtained by three different electric potentials of the electrospinning processes were  $358 \pm 84$ ,  $342 \pm 41$  and  $361 \pm 125$  nm of fiber a), b), and c) respectively. The data was shown in Figure 4.4.

The best electric potential condition of eletrospinning process in this experiment was 20 kV.



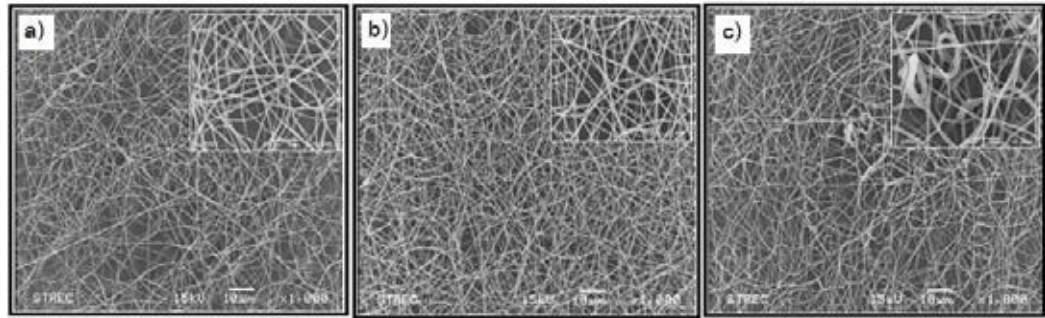


**Figure.4.4** SEM micrographs of 10:90:0 weight ratio of PVA/Schiff's reagent/Milli-Q water electrospun fiber under constant flow rate of 0.1 mL/hr and the distance between needle and collector of 25 cm using following processing conditions a) 15 kV, b) 20 kV, and c) 25 kV. Original magnification of 1,000 x and inset 5,000 x.

#### 4.1.2.3 Effect of the distance between needle and collector

The effects of the distances between the needle tip and the collector on morphology and fiber size diameter were investigated. Technically, the distance between the needle tip and the collector affects the evaporation time of solvent and acid. Increasing the distance between the needle tip, or the spinneret, and the collector usually has two effects on fiber formation process. Firstly, it reduce the strength of applied electric field, which in turn, lessens the amount of charged induced on polymer jet, and thus the force exerted on the polymer charged jet resulting in lesser degree of the charged jet elongation and greater fiber size. Increasing the collectiong distance also allow more space for the charged jet to elongate and more time for the solvent to evaporate. Therefore in some cases, this can lead to a smaller fiber size [30]. In this study, three different distances of 15, 20, and 25 cm were studied.

Figure 4.5 shows SEM micrographs of the blended PVA/Schiff's reagent/Milli-Q water at 10/90/0 % w/w ratio, and the electric field of 20 kV and the flow rate of 0.1 mL/hr. The diameter of electrospun fiber are  $367 \pm 110$ ,  $351 \pm 78$  and  $342 \pm 41$ , respectively. This observation is in agreement with the previous work. Therefore, we chose distance gap of 25 cm because it delivered a fine morphology, more uniform, and smallest diameter size comparing to the distance of 15 and 20 cm.

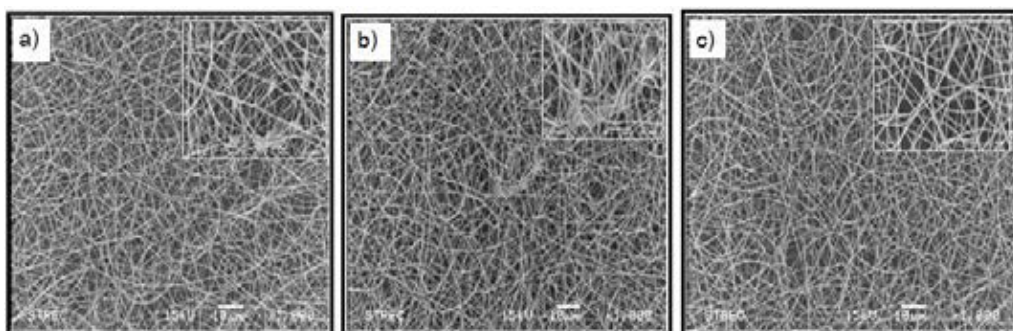


**Figure.4.5** SEM micrographs of 10:90:0 weight ratio of PVA/Schiff's reagent/Milli-Q water electrospun fiber under constant flow rate of 0.1 mL/hr and electric field of 20 kV using following processing conditions a) 15 cm, b) 20 cm, and c) 25 cm. Original magnification 1,000x and inset 5,000x.

Based on our finding, PVA was used as the sensor media because higher amount of PVA electrospun fiber with smaller size can be fabricated in the reasonable spinning time. The appropriate weight ratio of PVA/Schiff's reagent/Milli-Q water is 10:90:0 % w/w. The suitable conditions of electrospinning process were flow rate of 0.1 mL/hr, electric field of 20 kV, and distance between needle and collector of 25 cm.

## **4.2 Sensor stability**

The stability toward heat and storage time of three different types of substrates containing same amount of Schiff's reagent: Schiff's reagent solution, film sensor, and electrospun sensor were monitored. The Schiff's reagent solution was used in order to observe the changes before testing with sensors. The fault positive of the sensor, the change in color of sensor to violet without any exposure to formaldehyde gas, is the goal of this study. The absorbance at 580 nm was measured by using UV-visible spectrophotometer for the film sensor and Schiff's reagent and optic-fiber spectrophotometer for electrospun fiber mat.

### **4.2.1 Thermal stability**

The thermal stability of these three substrates was studied by controlling the system at 40, 50, 60, and 70 °C for 1-12 hours.

#### **4.2.1.1 Schiff's reagent**

Based on the increase in the absorbance at 580 nm, the increases in absorbance value at 580 nm were smaller for solutions kept at temperatures below 60°C comparing to the one kept at 70°C. Therefore, the stability of the Schiff's reagent solution at the temperature below 60°C was found to be fairly stable over 12 hours comparing to the solution kept at 70°C (Figure 4.6).

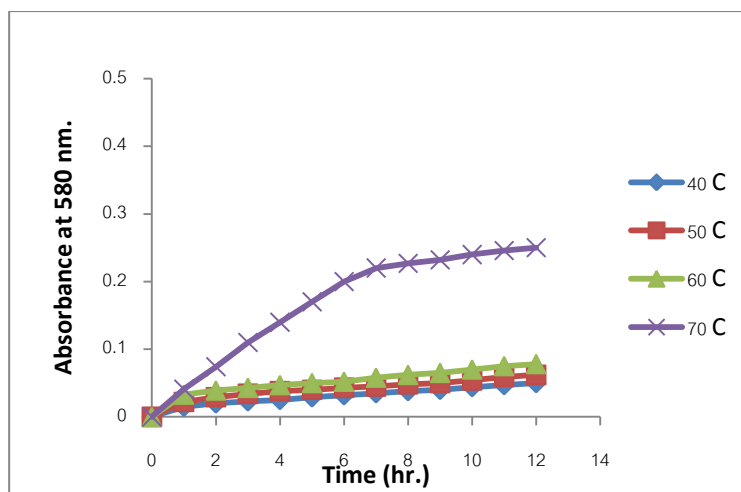


**Figure 4.6** The thermal stability of Schiff's reagent solution at various temperatures of 40, 50, 60, and 70 °C.

#### 4.2.1.2 Film sensor

Based on the observation in section 4.2.1.1 that the solution was stable at temperature below 70°C, the stability of film sensor was studied only at 60 and 70 °C. Therefore, the stability of film sensor at the temperature 60°C was found to be fairly stable over 12 hours comparing to the film kept at 70°C as shown in Figure 4.7.

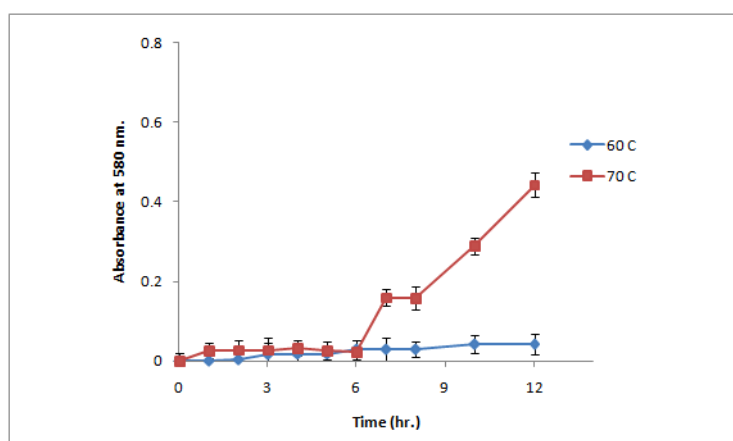


**Figure 4.7** The thermal stability of film at temperatures of 60 and 70 °C.

### 4.2.1.3 Electrospun sensor

From Figure 4.8, The electrospun fiber mat shows slight increase in absorbance value at 580 nm. However, the film color still remain white (data are not shown here) The smaller change in absorbance was observed on electrospun fiber sensor mat comparing to film sensor is due to the smaller amount of Schiff's reagent in the electrospun mat.

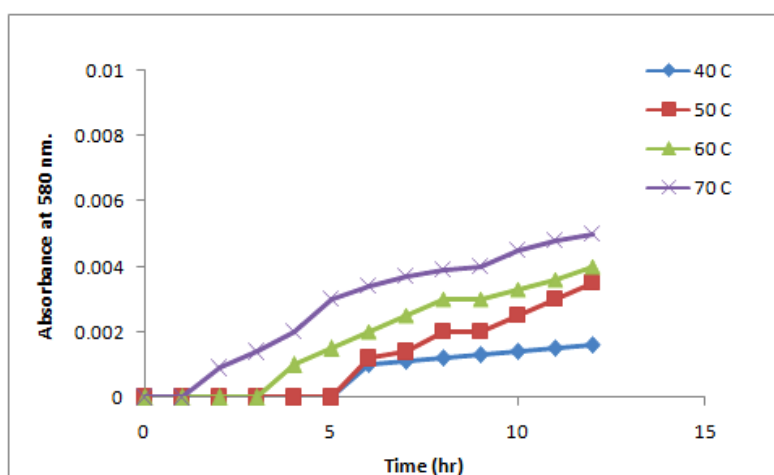


**Figure 4.8** The thermal stability of the electrospun fiber mats at 40, 50, 60, and 70 °C.

### 4.2.2 Storage Time

The stability study at room temperature is to observe the fault positive that might occur to the three different types of samples after kept at the room temperature which varied between 26-28°C for 30 days.

#### 4.2.2.1 Schiff's reagent solution

After 30-day storage time, the increase in absorbance at 580 nm was seen as shown in Figure 4.9. However, the color of Schiff's reagent became dark yellow and no violet color was observed (Figure 4.10 (a) and (b)). Furthermore, the dark yellow solution could detect the formaldehyde gas as shown in Figure 4.9 (c). Therefore, the Schiff's reagent can be used as sensing compound after 30-day storage.

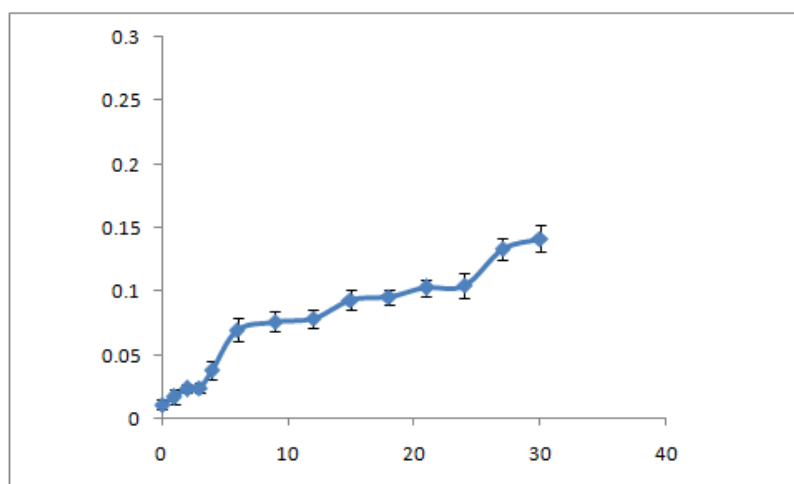


**Figure 4.9** The time stability of Schiff's solution. between 1-30 days

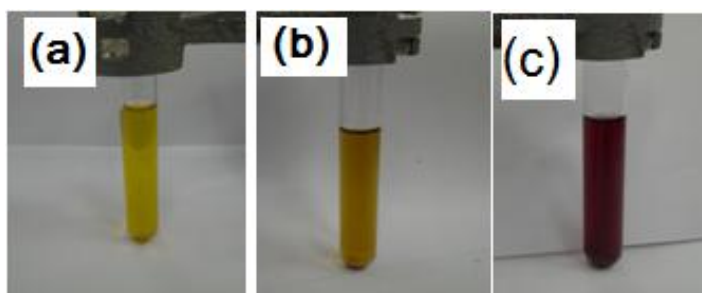


**Figure 4.10** The time stability of Schiff's solution on a) first day, b) day 30<sup>th</sup> and c) solution of day 30<sup>th</sup> that exposed to formaldehyde gas

#### 4.2.2.2 Film sensor

Although the increase in absorbance at 580 nm of a film sensor kept at room temperature in open atmosphere for over 30 days was found (Figure 4.12), the color of the film still remained yellow but got darker and no violet color was observed as shown in Figure 4.11 (a and b). Moreover, it still can be used as sensor for formaldehyde gas as seen in Figure 4.11 c). Therefore, the 30-days old film could be used as formaldehyde sensor.

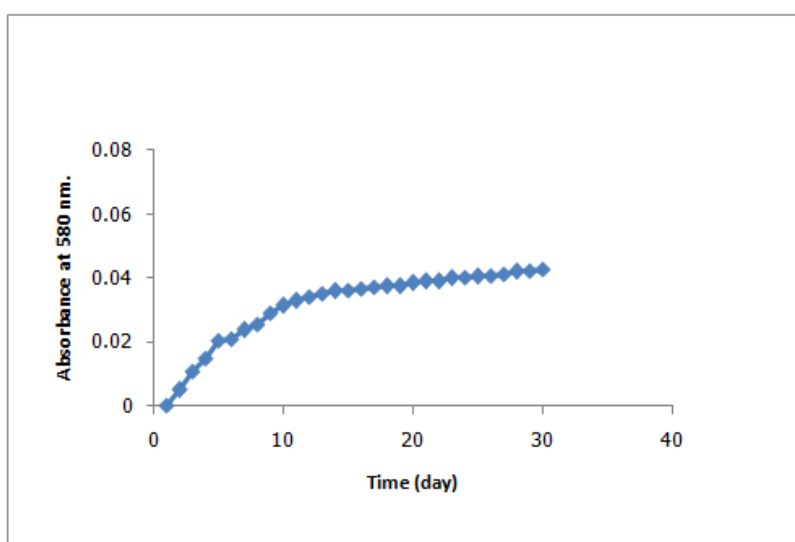


**Figure 4.11** The stability of film sensor ver -30 days storage

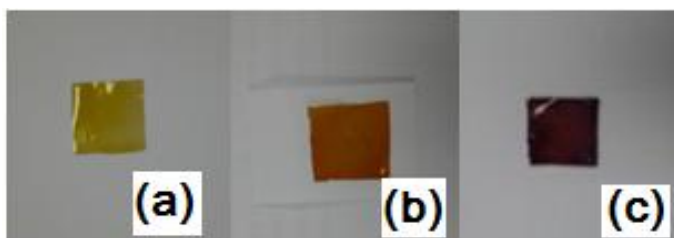


**Figure 4.12** The time stability of film a) 1 day, b) 30 days, c) film of day 30 that already exposed to generated formaldehyde gas

### 4.3 Process of generating formaldehyde gas

The generating formaldehyde gas process was described in section 3.6. The content of aldehyde gas was determined based on the reaction between acetylacetone solution and formaldehyde gas as shown in Figure 4.13. The product content was measured by UV-visible Spectrophotometer at 412 nm.

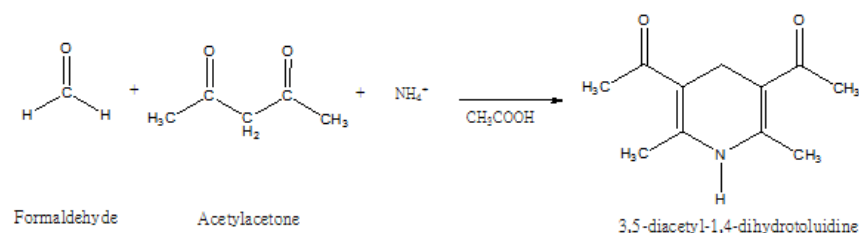


**Figure 4.13** Reaction of formaldehyde and acetylacetone solution [11].

The 37% w/v of formaldehyde solution were used for the formaldehyde gas generation. First, the reaction time between acetylacetone solution and formaldehyde gas and suitable working time were evaluated. Then, the effect of temperature and stirring rate of generated formaldehyde gas were optimized.

#### 4.3.1 Reaction time of formaldehyde and acetylacetone

The absorbance value of acetylacetone solution and formaldehyde gas was recorded by UV-visible spectrophotometer at 412 nm between the time periods of 0 to 60 minutes. The absorbance signal was increased from 1-15 minutes, after 15 minutes passed it remained constant as shown in Figure 4.14. Therefore, in this work the reaction time of 20-60 minutes was used.



The plot in Figure 4.14 was plot between the absorbance value at 412 nm after deducted with the absorbance of acetylacetone solution (blank) versus reaction time.

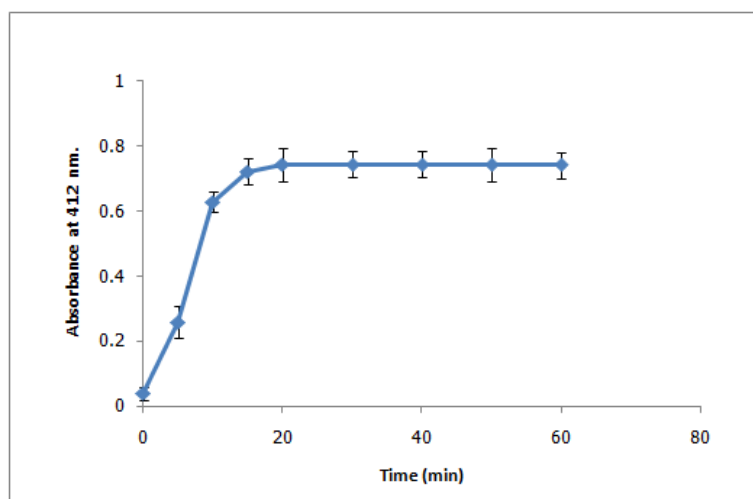


**Figure 4.14** Reaction time between generated formaldehyde gas and acetylacetone solution

### 4.3.2 Working time

From Figure 4.15, the content of generated formaldehyde gas was found to increase with the generating time and it reached the highest amount after 10 minutes and remained constant until 82 minutes passed. Therefore, the working time between 15-80 minutes was chosen for further study.

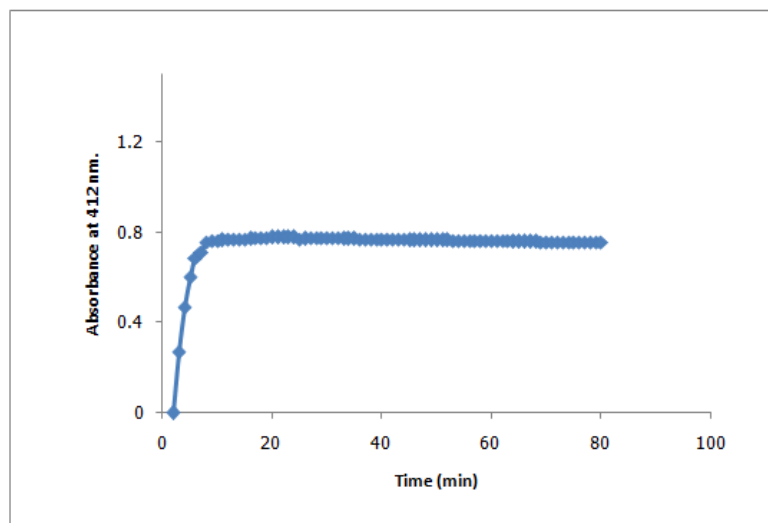


**Figure 4.15** Working time of generated formaldehyde gas system

### 4.3.3 Effect of temperature

In this part, the suitable temperature to generate a formaldehyde gas was evaluated. The temperature at 50 °C is suitable for generating gas because the highest amount of formaldehyde gas was generated at this temperature. (Figure 4.16)

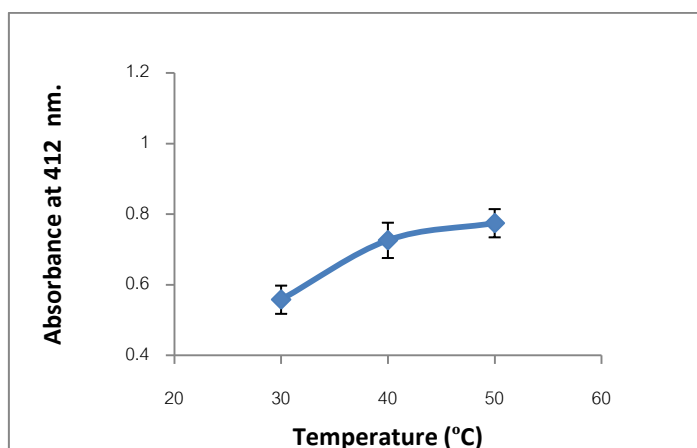


**Figure 4.16** Absorbance value of generated formaldehyde gas at various temperatures

#### 4.3.4 Effect of stirring rate

In this section, the various stirring rate was studied at 0, 100, 380, 660, and 940 rpm, respectively. From Figure 4.17, the more amount of formaldehyde gas was generated when the solution was stirred. However, the increase in the stirring rate has no effect on the evaporation of formaldehyde gas. The suitable stirring rate could be at any value between 100, 380, 660, and 940 rpm. Therefore, the stirring rate of 100 rpm was used in this work.

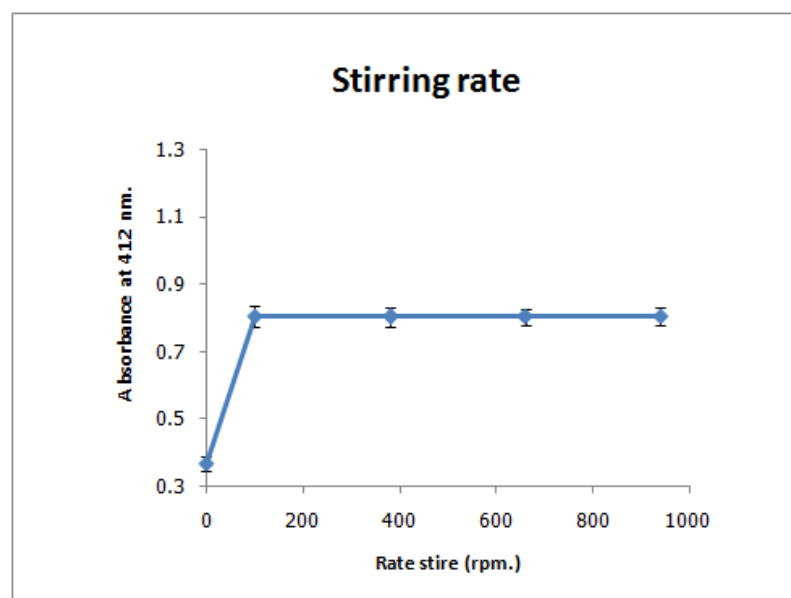


**Figure 4.17** Absorbance value of generated formaldehyde gas at various stirring rate

The working condition to generate formaldehyde gas from a 200 mL of 37% w/v of formaldehyde solution is 100mL/min flow rate of nitrogen gas as a carrier, 50 °C of formaldehyde solution and 100 rpm stirring rate.

#### 4.4 Concentration of generated formaldehyde gas

In order to quantify the formaldehyde gas in the study, the reaction between acetone with formaldehyde gas was chosen and the study was performed as described in the section 3.7.

##### 4.4.1 Calibration curve of the acetylacetone solution and formaldehyde solution

Due to the limit of working condition, the study in this section was performed only one time. The calibration curve of the acetylacetone solution and concentration of formaldehyde solution at 50, 100, 200, 500, 1000, 1500, and 2000  $\mu\text{g/L}$  were plot curve resulting to equation ;  $y = 0.003x + 0.147$ ,  $R^2 = 0.987$

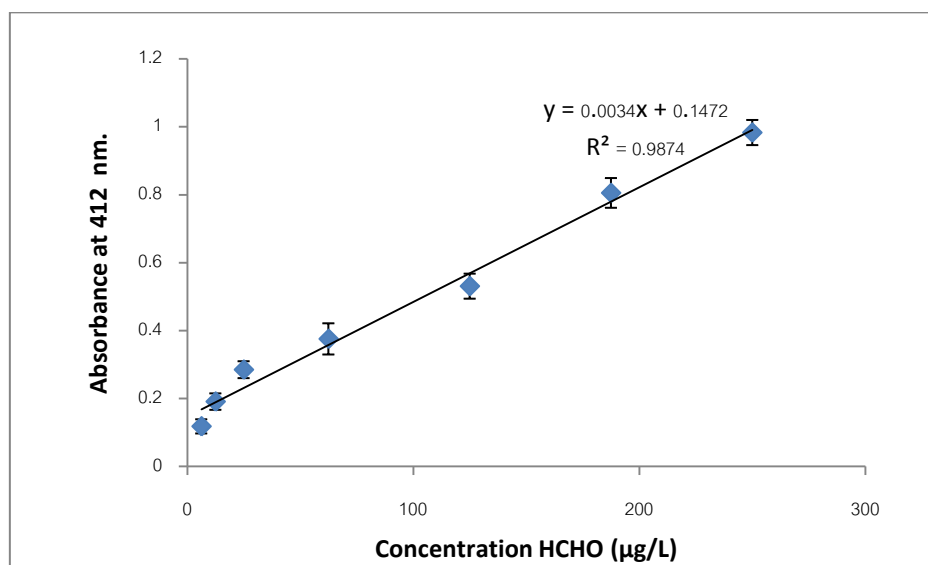


**Figure 4.18** Calibration curve of a acetylacetone solution versus various concentration formaldehyde solutions.

#### 4.4.2 Calculated concentration of formaldehyde gas generated

The concentration of pure formaldehyde gas was determined according to the section 3.7. The absorbance at 412 nm is 0.803 AU (data are not shown here). Using linear regression equation ( $y = 0.003x + 0.147$ ), the concentration of pure formaldehyde gas (100%) equals to 218.7  $\mu\text{g/L}$  in solution. After accounting the dilution factor, the concentration of formaldehyde gas is 1749.6  $\mu\text{g/L}$  in solution. Then the content of formaldehyde gas in 7 mL of acetylacetone solution was calculated, which equal to the amount of formaldehyde gas in 100 mL of gas stream. Then, the amount of formaldehyde gas equals 12.247  $\mu\text{g}$  in 100 mL (122.47  $\mu\text{g/L}$  in gas stream)

As described in section 3.8, the formaldehyde gas generated in the previous section was mixed with nitrogen gas at various mixing ratio. The concentration of formaldehyde gas for each mixing ratio was calculated and shown in Table 4.3.

**Table 4.2** The calculated of generated formaldehyde gas concentrations

Mixing ratio of generated gas : Nitrogen gas (mL/ min)	% of generated gas	Concentration of generated formaldehyde gas ( $\mu\text{g/L}$ in gas stream)
100 : 100	50%	61
100 : 80	55%	67
100 : 60	62%	76
100 : 40	71%	87
100 : 20	83%	102
100 : 00	100%	122

## 4.5 Sensor performance testing

### 4.5.1 Electrospun sensor

The electrospun sensor performance was tested at various concentration of the formaldehyde gas. After electrospun sensor exposed to formaldehyde gas for 24 hours, the change in color of the electrospun fibers to violet was observed. As the concentration of the formaldehyde gas increased, more violet appeared, as shown in Figure 4.19.

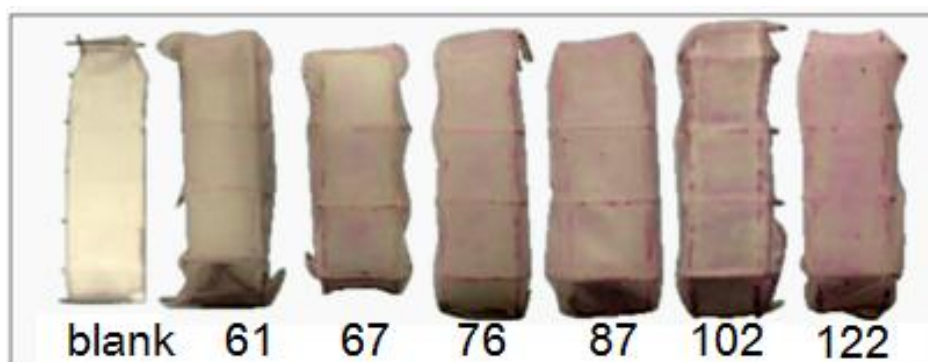


**Figure 4.19** Images of the 10:90:0 mass ratio of PVA, Schiff's reagent and Milli-Q water electrospun fiber sensor after exposure to formaldehyde gas at concentration of 61, 67, 76, 87, 102 and 122  $\mu\text{g/L}$  (blank: sensor before incorporating into the testing system)

The absorbance at 580 nm was also recorded using optic-fiber spectrophotometry. The data was shown in Figure 4.20.

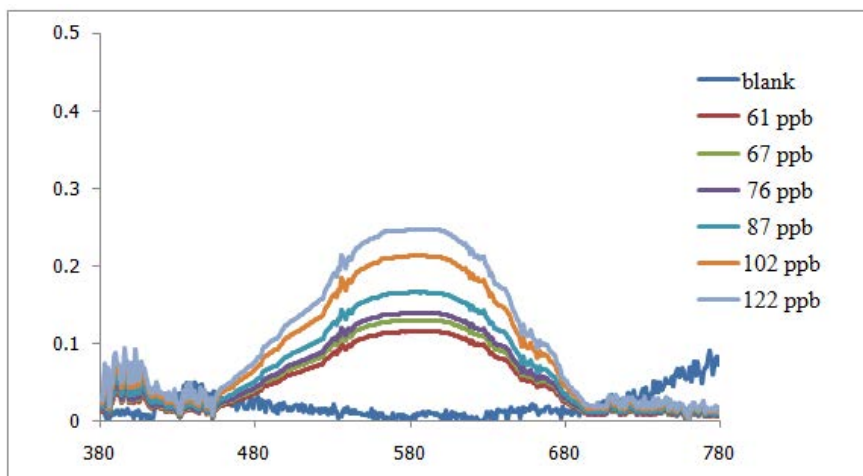


**Figure 4.20** The absorbance spectra of the 10:90:0 %w/w blended PVA, Schiff's reagent and Milli-Q water electrospun sensor after exposure to formaldehyde gas at concentration of 61, 67, 76, 87, 102 and 122  $\mu\text{g/L}$  (blank: sensor before incorporating into the testing system)

The plot of an absorbance value at 580 nm versus a concentration of formaldehyde gas in this experiment was found to be linear. Therefore, our sensor could be used to detect the formaldehyde gas concentration ranging from 61-122  $\mu\text{g/L}$  (Figure 4.21). However, further study on more sample and more run are needed to confirm our finding.

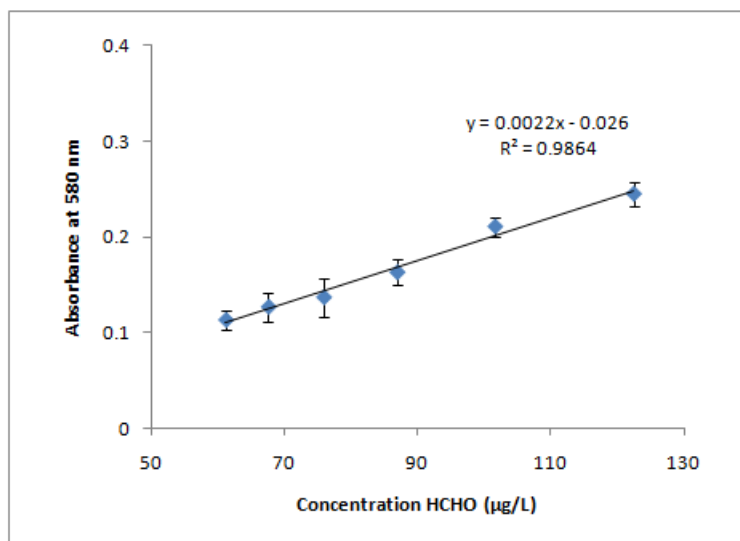


**Figure 4.21** The relationship between absorbance value at 580 nm and various concentration formaldehyde: 61, 67, 76, 87, 102 and 122 µg/L.

#### 4.5.2 Film sensor

After a film sensor was exposed to formaldehyde gas with various concentrations for 24 hours, the change in color of the film sensor from yellow to violet was observed. As the concentration of the formaldehyde gas increased, more violet appeared, as shown in Figure 4.22.



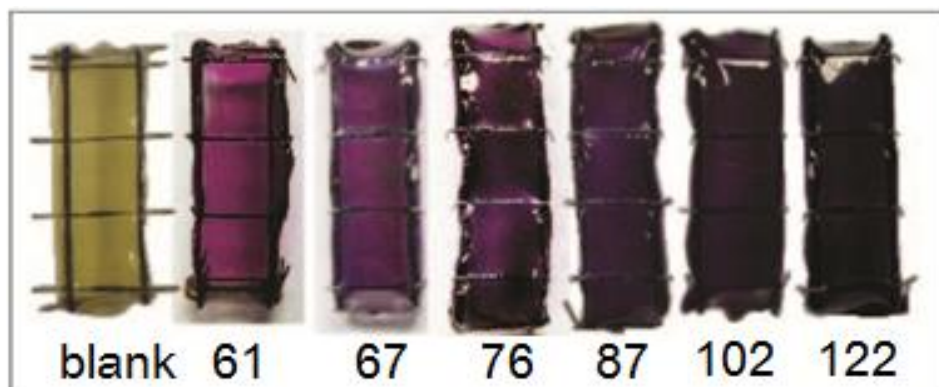


**Figure 4.22** The absorbance spectra of the 10:90:0 %w/w blended PVA, Schiff's reagent and Milli-Q water film sensor after exposure to formaldehyde gas at concentration of 61, 67, 76, 87, 102 and 122  $\mu\text{g/L}$  (blank: sensor before incorporating into the testing system)

The absorbance value at 580 nm was found to increase as the concentration of the formaldehyde gas was increased as shown in Figure 4.23.

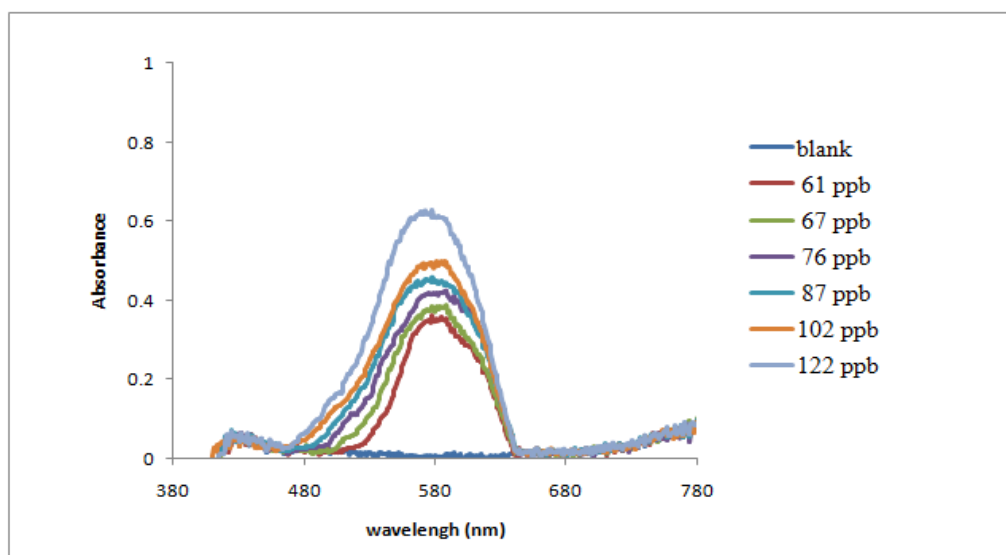


**Figure 4.23** The absorbance spectra of the 10:90:0 %w/w blended PVA, Schiff's reagent and Milli-Q water film sensor after exposure to formaldehyde gas at concentration of 61, 67, 76, 87, 102 and 122  $\mu\text{g/L}$  (blank: sensor before incorporating into the testing system)

The linear curve between an absorbance value at 580 nm and concentration of generated formaldehyde gas ranging from 61 - 122  $\mu\text{g L}^{-1}$  was found (Figure 4.25).

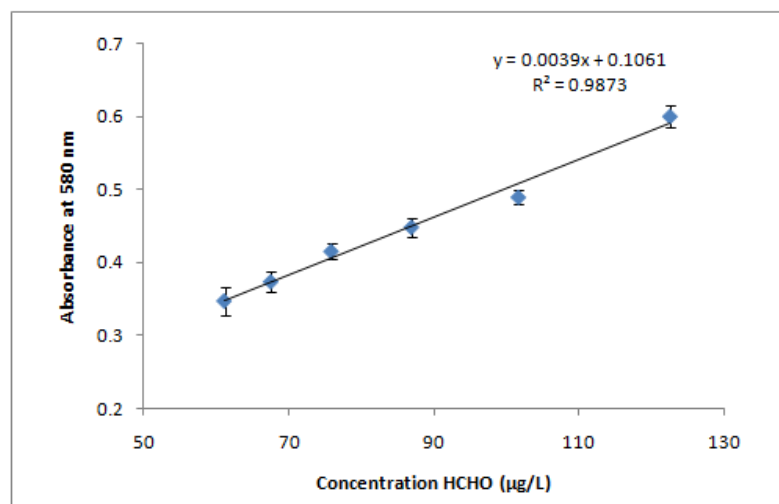


**Figure 4.24** The absorbance value at 580 nm and various concentration formaldehyde of 61, 67, 76, 87, 102 and 122  $\mu\text{g/L}$ , (blank: sensor before incorporating into the testing system).

The performance of the electrospun sensor comparing to the film sensor was found to be less than the film sensor. This might be due to the higher amount of Schiff's reagent in the film sensor.

#### **4.6 Precision of sensor performance**

The precision of sensor performance was evaluated on both electrospun and film sensors. The precision of sensor performance was tested in three different days using one sample per day and each sample containing 3 frames. The sensor was exposed with pure formaldehyde generated gas as concentration range of 120.96 - 122.64  $\mu\text{g/L}$ . The results were summarized in Table 4.4. The relative standard deviation (RSD) of the absorbance at 580 nm of both electrospun sensor and film sensor were 1.22% and 2.66%, respectively.

**Table 4.3** The Absorbance at 580 nm of the electrospun and film sensor tested with pure formaldehyde gas as calculated concentration range of 120.96 - 122.64  $\mu\text{g/L}$ .

Day	Frame of sensor	Absorbance at 580 nm	
		Electrospun fiber	Film
1	1	0.246	0.605
	2	0.245	0.602
	3	0.244	0.593
2	4	0.248	0.610
	5	0.250	0.631
	6	0.249	0.618
3	7	0.241	0.581
	8	0.240	0.587
	9	0.243	0.590
	<b>Mean</b>	0.245	0.602
	<b>SD</b>	0.003	0.016
	<b>% RSD</b>	1.22	2.66

## CHAPTER V

### CONCLUSION

The fabricated optical sensors are made of a blended PVA/Schiff's reagent/Milli-Q water using an electrospinning technique. The electrospun fiber was fabricated in regular morphology, well-distributed, and the diameter is between  $342 \pm 41$  nm. The morphology of electrospun fibers were characterized by using the Scanning Electron Microscope (SEM). The factors of mass ratio, electrical potential and a distance between the needle and the collector affect the morphology and diameter of electrospun fiber. Increasing the electric potential and the distance between a needle and a collector, result the fiber diameter to decrease. The mass ratio of 10:90:0, the distance of 25 cm, the electrical potential 20 kV, and flow rate controlled at 0.1 mL/hr was selected as the optimum condition for electrospinning process. In the meantime, the optical sensor using casting technique was using the same polymer solution with mass ratio of 10:90:0 of the blended PVA/Schiff's reagent/Milli-Q water which are consider the best solution to produce an electrospun fiber.

The stability of three different types substrates containing same Schiff's reagent were separate both of thermal and time stability for studied, In Thermal stability section found that, Schiff's reagent solution and film were unstable at 70 °C. In Time stability section found that Schiff's reagent solution was unstable when placed in room temperature for 30 days.

The process of generating formaldehyde gas system is to heat the formaldehyde solution, formaldehyde solution will turn to formaldehyde gas by using nitrogen gas as a carrier gas to carry the generated gas in to the sensing chamber.

The factors affecting the concentration of the generated formaldehyde gas in generating gas system are temperature, and stirring rate of generating formaldehyde gas process. The optimum conditions of generating formaldehyde gas in generating gas system were 37% w/v of formalin concentration, 50 °C, and 100 rpm stirring rate of generating formaldehyde gas process.

The optical sensors were tested with generated formaldehyde gas with the concentration of 61–122 µg/L. It was founded that when the electrospun and film sensor exposed with formaldehyde gas, its color changes to violet, when increasing the concentration of formaldehyde gas, result in more violet to be appeared. The sensor exposed with generated formaldehyde gas was analyzed by using an optic-fiber spectrophotometer. It was found that, the absorbance value at 580 nm increased as the violet appeared.

Finally, the optical sensor was successfully developed by using a blended PVA/Schiff's reagent/Milli-Q water via electrospinning process and casting process for formaldehyde gas sensing. The new sensors can detect formaldehyde gas in various concentrations by naked-eyes for analysis. The sensor was simply prepare, inexpensive, portable, and non toxicity.

**Suggestions for further work**

The suggestion for the further work is to solve the equalization of the weight of the electrospun sensor and the weight of the film sensor, so it could be compare its performance without unequal weight. In addition, the proposed sensor should be further studied on the limit of detection (LOD) and response time of the sensor. Finally the sensor should be tested with real environment such as the hospital, factory, houses, and school.

## REFERENCES

- [1] Tang, X.; Bai, Y.; Duong, A.; Smith, M. T.; Li, L.; Zhang, L., Formaldehyde in China: production, consumption, exposure levels, and health effects. Environment International 35 (2009): 1210-1224.
- [2] Kawamura, K.; Kerman, K.; Fujihara, M.; Nagatani, N.; Hashiba, T.; Tamiya, E., Development of a novel hand-held formaldehyde gas sensor for the rapid detection of sick building syndrome. Sensors and Actuators B: Chemical 105 (2005): 495-501.
- [3] Charles, K.; Magee, R.; Won, D., Indoor Air Quality Guidelines and Standards. National Research Council Canada (2005): 10-25.
- [4] Flueckiger, J.; Ko, F. K.; Cheung, K. C., Microfabricated formaldehyde gas sensors. Sensors 9 (2009): 9196-9215.
- [5] Kumagai, S.; Sasaki, K.; Shimizu, Y.; Takeda, K., Formaldehyde and acetaldehyde adsorption properties of heat-treated rice husks. Separation and Purification Technology 61 (2008): 398-403.
- [6] Lee, K. J.; Shiratori, N.; Lee, G. H.; Miyawaki, J.; Mochida, I.; Yoon, S.-H.; Jang, J., Activated carbon nanofiber produced from electrospun polyacrylonitrile nanofiber as a highly efficient formaldehyde adsorbent. Carbon 48 (2010): 4248-4255.
- [7] Oehme, I.; Wolfbeis, O., Optical chemical sensors for the determination of heavy metal ions, Mikrochimica Acta 126 (1997): 177-192.
- [8] Pucheler, H.; Meloan, S., On Schiff's base and aldehyde- fuchsin: a review from H. Schiff to R.D. Lillie. Histochemistry 72 (1987): 321-332
- [9] Suzuki, Y.; Nakano, N.; Suzuki, K., Portable sick house syndrome gas monitoring system based on novel colorimetric reagents for the highly selective and sensitive detection of formaldehyde. Environmental Science and Technology 37 (2003): 5695 - 5700.
- [10] Kawamura, K.; Kerman, K.; Fujihara, M.; Nagatani, N.; Hashiba, T.; Tamiya, E., Development of a novel hand-held formaldehyde gas sensor for the rapid detection of sick building syndrome. Sensors and Actuators B: Chemical 105 (2005): 495-501.



- [11] Maruo, Y. Y.; Nakamura, J.; Uchiyama, M., Development of formaldehyde sensing element using porous glass impregnated with  $\beta$ -diketone. Talanta 74 (2008): 1141-1147.
- [12] Maruo, Y. Y.; Nakamura, J.; Uchiyama, M.; Higuchi, M.; Izumi, K., Development of formaldehyde sensing element using porous glass impregnated with Schiff's reagent. Sensors and Actuators B: Chemical 129 (2008): 544-550.
- [13] Ding, B.; Wang, M.; Yu, J.; Sun, G., Gas sensors based on electrospun nanofibers. Sensors 9(2009): 1609-1624.
- [14] Wikipedia. Formaldehyde[Online]  
from: <http://en.wikipedia.org/wiki/Formaldehyde>. [2013, March 5]
- [15] Liteplo, R. G.; Beauchamp, R.; Meek, M.E.; Chénier, R., Formaldehyde geneva: the united nations environment programme. The international labour organization, and the world health organization (2002):1-74.
- [16] Wikipedia. Schiff's reagent. [Online]  
from: [http://en.wikipedia.org/wiki/Schiff\\_test](http://en.wikipedia.org/wiki/Schiff_test). [2013, March 5]
- [17] Hardonk, M.; Van Duijn, P., The mechanism of the Schiff reaction as studied with histochemical model systems. J. Histochem. Cytochem 12 (1964):748-751.
- [18] Robins, J. H.; Abram, s., The structure of Schiff reagent aldehyde adducts and the mechanism of the Schiff's reaction as determined by nuclear magnetic resonance spectroscopy. Can.J.chem 58(1980): 339-347.
- [19] Jagadeesh, B.V.; Satheesh, K.K.; Trivedi, D.C.; Murthy, V.R. Natarajan, T.S., Electrical Properties of Electrospun Fibers. Journal of Engineered Fibers and Fabrics 2 (2007): 25-31.
- [20] Renker, D. H.; Chun, I. Nanometre diameter fibres of polymer produced by electrospinning. Nanotechnology 7 (1996): 216-223.
- [21] Deitzel, J. M.; Kleinmeyer, J.; Harris, D.; Beck Tan, N. C.; The effect of processing variables on the morphology of electrospun nanofibers and textiles. Polymer 42 (2001): 261-272.

- [22] Ramakrishna, S.; Fujihara, K.; Teo, W.E.; Lim, T.C.; Ma, Z., An introduction to electrospinning and nanofibers. Singapore: World Scientific Publishing Co. Pte. Ltd., 2005.
- [23] Hohman, M. M.; Shin, M.; Rutledge, G.; Brenner, M. P., Electrospinning and electrically forced jets. II. Applications. Physics of Fluids 13 (2001): 2221-2236.
- [24] Bunkoed, O.; Davis, F.; Kanatharana, P.; Thavarungkul, P.; Higson, S. P. J., Sol-gel based sensor for selective formaldehyde determination. Analytica Chimica Acta 659 (2010): 251-257.
- [25] Zhang, C.; Wang, X.; Lin, J.; Ding, B.; Yu, J.; Pan, N., Nanoporous polystyrene fibers functionalized by polyethyleneimine for enhanced formaldehyde sensing. Sensors and Actuators B: Chemical 152 (2011): 316-323.
- [25] Sun, G.; Teng, H.; Zhac, C. Preparation of Ultrafine Water-soluble Polymers Nanofiber Mats *via* Electrospinning CHEM. RES. 26 (2010) : 318—322.
- [26] Hohman, M. M.; Shin, M.; Rutledge, G.; Brenner, M. P., Electrospinning and electrically forced jets. I. Stability theory. Physics of Fluids 13 (2001): 2201-2220.
- [27] Chowdhury, M.; and Stylios, G., Effect of experimental parameters on the morphology of electrospun Nylon 6 fibres. IJBAS: International Journal of Basic & Applied Sciences 10 (2012): 116-131.
- [28] Fong, H.; Chun, I. and D.; Reneker, H., Beaded nanofibers formed during electrospinning. Polymer 40(1999): 4585–4592.
- [29] Baji, A.; Mai, Y. W.; Wong, S. C.; Abtahi, M. Chen, P., Electrospinning of polymer nanofibers: Effects on oriented morphology, structures and tensile properties. Composites Science and Technology 70 (2010): 703–718.
- [30] Li, D.; Xia, Y., Electrospinning of nanofibers: reinventing the wheel. Advanced materials 16 (2004): 1151-1170.

## VITA

Miss Thitirat Lukboon was born on September 13, 1986 in Srisaket, Thailand. She graduated with a Bachelor of Science degree in Srinakarinwirot University in 2009. After that, she has been a graduated student at Program of Petrochemisty and Polymer Science, Faculty of Science Chulalongkorn University and become a member of Chromatography and Separation Research Unit. She finished her Master's degree of Science in 2012.